frontiers in Physiology

ORIGINAL RESEARCH
published: 25 February 2021
doi: 10.3389/fphys.2021.642237

Comprehensive Quantitative Proteome Analysis of *Aedes aegypti* Identifies Proteins and Pathways Involved in *Wolbachia pipientis* and Zika Virus Interference Phenomenon

Michele Martins[1†], Luis Felipe Costa Ramos[1†], Jimmy Rodriguez Murillo[2], André Torres[3], Stephanie Serafim de Carvalho[1], Gilberto Barbosa Domont[1], Danielle Maria Perpétua de Oliveira[1], Rafael Dias Mesquita[1], Fábio César Sousa Nogueira[1], Rafael Maciel-de-Freitas[4]* and Magno Junqueira[1]*

[1] Departamento de Bioquímica, Instituto de Química, Universidade Federal do Rio de Janeiro, Rio de Janeiro, Brazil, [2] Division of Chemistry I, Department of Medical Biochemistry and Biophysics, Karolinska Institute, Stockholm, Sweden, [3] Carlos Chagas Filho Biophysics Institute, Universidade Federal do Rio de Janeiro, Rio de Janeiro, Brazil, [4] Laboratório de Mosquitos Transmissores de Hematozoários, Instituto Oswaldo Cruz, Fiocruz, Rio de Janeiro, Brazil

Zika virus (ZIKV) is a global public health emergency due to its association with microcephaly, Guillain-Barré syndrome, neuropathy, and myelitis in children and adults. A total of 87 countries have had evidence of autochthonous mosquito-borne transmission of ZIKV, distributed across four continents, and no antivirus therapy or vaccines are available. Therefore, several strategies have been developed to target the main mosquito vector, *Aedes aegypti*, to reduce the burden of different arboviruses. Among such strategies, the use of the maternally-inherited endosymbiont *Wolbachia pipientis* has been applied successfully to reduce virus susceptibility and decrease transmission. However, the mechanisms by which *Wolbachia* orchestrate resistance to ZIKV infection remain to be elucidated. In this study, we apply isobaric labeling quantitative mass spectrometry (MS)-based proteomics to quantify proteins and identify pathways altered during ZIKV infection; *Wolbachia* infection; co-infection with *Wolbachia*/ZIKV in the *A. aegypti* heads and salivary glands. We show that *Wolbachia* regulates proteins involved in reactive oxygen species production, regulates humoral immune response, and antioxidant production. The reduction of ZIKV polyprotein in the presence of *Wolbachia* in mosquitoes was determined by MS and corroborates the idea that *Wolbachia* helps to block ZIKV infections in *A. aegypti.* The present study offers a rich resource of data that may help to elucidate mechanisms by which *Wolbachia* orchestrate resistance to ZIKV infection in *A. aegypti,* and represents a step further on the development of new targeted methods to detect and quantify ZIKV and *Wolbachia* directly in complex tissues.

Keywords: proteome, quantitative, *Aedes aegypti*, *Wolbachia*, Zika virus, immune response

OPEN ACCESS

Edited by:
Jose Luis Ramirez, United States Department of Agriculture (USDA), United States

Reviewed by:
Valérie Choumet, Institut Pasteur, France
José Henrique M. Oliveira, Federal University of Santa Catarina, Brazil

***Correspondence:**
Magno Junqueira
magnojunqueira@iq.ufrj.br
Rafael Maciel-de-Freitas
freitas@ioc.fiocruz.br

[†] These authors have contributed equally to this work

Specialty section:
This article was submitted to Invertebrate Physiology, a section of the journal Frontiers in Physiology

Received: *15 December 2020*
Accepted: *04 February 2021*
Published: *25 February 2021*

Citation:
Martins M, Ramos LFC, Murillo JR, Torres A, de Carvalho SS, Domont GB, de Oliveira DMP, Mesquita RD, Nogueira FCS, Maciel-de-Freitas R and Junqueira M (2021) Comprehensive Quantitative Proteome Analysis of Aedes aegypti Identifies Proteins and Pathways Involved in Wolbachia pipientis and Zika Virus Interference Phenomenon. Front. Physiol. 12:642237. doi: 10.3389/fphys.2021.642237

HIGHLIGHTS

- The abundance of ZIKV polyprotein is reduced in the presence of *Wolbachia*.
- Shotgun proteomics quantifies ZIKV and *Wolbachia* proteins directly in tissues.
- *Wolbachia* regulates proteins involved in ROS production.
- *Wolbachia* regulates humoral immune response and antioxidant production.
- Metabolism and detoxification processes were associated with mono infections.

INTRODUCTION

Zika virus (ZIKV) is a single-stranded RNA virus that belongs to the *Flavivirus* genus and Flaviviridae family. Originally discovered in a primate from the Zika forest in Uganda in 1947, remained unimportant for public health until the beginning of the 20th century (Dick et al., 1952). In 2014, ZIKV emerged in the Pacific islands and a few years later invaded the Americas, leading the World Health Organization to claim a global public health emergency due to its association with microcephaly in newborns and Guillain-Barré syndrome, neuropathy, and myelitis in children and adults (Campos et al., 2015; Barreto et al., 2016). As of May 2017, around 75% of inhabitants of the Yap Islands were infected with ZIKV, but no microcephaly was recorded. Whilst in Brazil more than 220,000 cases were recorded and more than 2,600 newborns had birth defects like microcephaly and other neuropathies (Baud et al., 2017).

The mosquito *Aedes aegypti* is the primary vector of ZIKV worldwide (Chouin-Carneiro et al., 2016; Ferreira-de-Brito et al., 2016). To date, no antivirus therapy or vaccines are available to mitigate ZIKV transmission, which increases the urgency for effective methods targeting the mosquito vector to reduce the burden of arboviruses as ZIKV. Among such strategies, the use of the maternally inherited endosymbiont *Wolbachia pipientis* has gained attention recently. The bacterium *Wolbachia* is naturally found in around 60% of arthropod species. Although *Wolbachia* does not naturally infect *A. aegypti*, some strains were transinfected by microinjection into this mosquito species with the further discovery of their pathogen-blocking properties (Moreira et al., 2009; Aliota et al., 2016; Dutra et al., 2016). The rationale underlying a mass release of *Wolbachia* infected mosquitoes is to replace the local *A. aegypti* population. Usually, it has high vector competence to arboviruses, like ZIKV, while the *Wolbachia* transinfected mosquitoes have reduced susceptibility and decreased transmission (Hoffmann et al., 2011). This approach is currently ongoing in at least 12 countries and the first communications showing its impact on disease transmission decrease are being revealed (Nazni et al., 2019; Indriani et al., 2020; Ryan et al., 2020).

The mechanisms which are orchestrated by *Wolbachia*, conferring resistance to arboviruses infection remain to be elucidated, however, it has been assigned to the activation of the mosquito immune system, down-regulation of genes that encode proteins or receptors necessary to the virus binding and depletion of host's resources essentials to the virus life cycle (Ford et al., 2020). When infected with *Wolbachia*, the mosquito Toll pathway is activated through the increase of reactive oxygen species (ROS), resulting in the production of antimicrobial peptides like cecropin (Pan et al., 2012). The gene expression modulation of tubulin, insulin receptors, and other genes seems to hinder the virus infection (Haqshenas et al., 2019; Paingankar et al., 2020). Also, it has been proposed that the lipids are relevant to *Wolbachia* infection. While one study implies it competes with the host's lipid resources (mainly cholesterol), others suggest it modulates the lipid production which can have a role blocking virus replication (Geoghegan et al., 2017; Koh et al., 2020; Manokaran et al., 2020).

Protein quantification on a genome-wide scale allows a systemic bird's-eye view of protein variation and pathway regulation under different conditions and samples (Choudhary and Mann, 2010). Therefore, it helps to highlight some features and emergent properties of complex systems, which could be obscured when the analysis is performed only from a reductionist point of view. In this way, mass spectrometry (MS)-based proteomics, together with robust bioinformatic tools, allows the formulation of more ambitious hypotheses due to the possibility of generating large and detailed datasets. Reliable large-scale protein quantification can be achieved using isobaric labeling and shotgun proteomics (Pappireddi et al., 2019). Several quantitative methods have already been successfully applied in insects to access differentially regulated proteins (De Mandal et al., 2020; García-Robles et al., 2020; Serteyn et al., 2020). The *A. aegypti* infection with Mayaro virus or microsporidian parasites have already been studied (Duncan et al., 2012; Vasconcellos et al., 2020) and a previous descriptive work was based on comparing the proteome of *A. aegypti* female heads during blood and sugar meals conditions (Nunes et al., 2016).

Here, we use an isobaric labeling-based quantitative proteomic strategy to interrogate the interaction between the *Wolbachia w*Mel strain and ZIKV infection in *A. aegypti* heads and salivary glands. *Wolbachia* is present in several tissues and organs in *A. aegypti* mosquitoes, with higher density in ovaries and tissues on the head and anterior part of the thorax, like the ommatidia cells, brain, salivary glands, and cardia (Moreira et al., 2009). To the best of our knowledge, this is the most complete proteome of *A. aegypti* reported so far, with a total of 3,790 proteins identified, corresponding to 25.75% of total protein-coding genes. This work includes the identification and quantification of several peptides from the ZIKV and 323 *Wolbachia* proteins in a complex sample tissue, paving the way to the development of sensitive approaches to detect and quantify the ZIKV and *Wolbachia* directly in the *A. aegypti* tissue via MS. Moreover, we describe and discuss proteins and pathways altered in *A. aegypti* during ZIKV infections, *Wolbachia* infections, co-infection *Wolbachia*/ZIKV, and compared with no infection.

MATERIALS AND METHODS

Mosquitoes

To access the effects of ZIKV and *Wolbachia* infection on *A. aegypti* proteome, we used mosquitoes from two different sites in Rio de Janeiro (Rio de Janeiro State, Brazil): Tubiacanga (22°47′06″S; 43°13′32″W) and Porto (22°53′43″S, 43°11′03″W), distant 13 km apart from each other. Tubiacanga was selected to represent an area in which mosquitoes have *Wolbachia* (*w*Mel strain) since it is the first site in Latin America with an established invasion (>90% frequency) (Garcia et al., 2019). Porto represents a *Wolbachia* free area. Eggs were collected through 80 ovitraps (Codeço et al., 2015) installed every 25–50 m each other in both sites. Ovitraps were placed over an extensive geographic area to ensure we captured the local *A. aegypti* genetic variability, collecting at least 500 eggs per site. The eggs were hatched and the mosquitoes were maintained at the insectary under a relative humidity of 80 ± 5% and a temperature of 25 ± 3°C, with *ad libitum* access to a 10% sucrose solution. The experimental infection was performed with mosquitoes from the F1 generation.

Viral Strain

Aedes aegypti females were orally infected with the ZIKV strain Asian genotype isolated from a patient in Rio de Janeiro (GenBank accession number KU926309). Previous reports have shown high infectivity of this ZIKV isolate to Rio de Janeiro *A. aegypti* populations, including Porto, which had 100% infected females after receive an infective blood meal (Fernandes et al., 2016; da Silveira et al., 2018; Petersen et al., 2018). Viral titers in supernatants were previously determined by serial dilutions in Vero cells, expressed in plaque-forming units per milliliters (PFU/ml). All the assays were performed with samples containing 3.55×10^6 PFU/ml. Viral stocks were maintained at −80°C until its use.

ZIKV Infection

Sugar supply was removed 36-h before mosquitoes were challenged with the infective blood meal to increase female's avidity. Six–seven days old inseminated *A. aegypti* females from each of the two populations (Tubiacanga and Porto) were separated in cylindrical plastic cages for blood-feeding. Oral infection procedures were performed through a membrane feeding system (Hemotek, Great Harwood, United Kingdom), adapted with a pig-gut covering, which gives access to human blood. The infective blood meals consisted of 1 ml of the supernatant of infected Vero cell culture, 2 ml of washed rabbit erythrocytes, and 0.5 mM of adenosine triphosphate (ATP) as phagostimulant. The same procedure and membrane feeding apparatus were used to feed control mosquitoes, i.e., control insects received a noninfectious blood meal, with 1 ml of Vero cell culture medium replacing the viral supernatant (therefore, with no ZIKV), 2 ml of washed rabbit erythrocytes, and 0.5 mM of ATP as phagostimulant. After the experimental infection, we had a total of 152 *A. aegypti* females.

Ethical Approval

The maintenance of *A. aegypti* colonies with *Wolbachia* in the lab were achieved by offering blood obtained from anonymous donors from the blood bank of the Rio de Janeiro State University, whose blood bags would be discarded due to small volume. We have no information on donors, including sex, age, and clinical condition, but the blood bank discards those bags positive for Hepatitis B, Hepatitis C, Chagas disease, syphilis, human immunodeficiency virus, and human T-cell lymphotropic virus. Before offering the blood for mosquitoes, it was screened for Dengue virus (DENV) using the Dengue NS1 Ag STRIP (Bio-Rad). The use of human blood was approved by the Fiocruz Ethical Committee (CAAE 53419815.9.0000.5248).

Protein Extraction for Proteomics

Proteins from a total of 152 *A. aegypti* females were processed, of which 39 were coinfected with *Wolbachia* and ZIKV (WZ); 36 non-infected (A); 35 infected with *Wolbachia* (W) only and 42 infected with ZIKV (Z). On 14 days post-infection, each mosquito head plus the salivary gland was separated from the body using needles and a scalpel blade which were sterilized after every single use (Schmid et al., 2017). Proteins were extracted by lysis with a buffer containing 7 M urea, 2 M thiourea, 50 mM HEPES pH 8, 75 mM NaCl, 1 mM EDTA, 1 mM PMSF, and protease/phosphatase inhibitor cocktails (Roche). Then, samples were vortexed, sonicated in a cold bath for 10 min and sonicated by the probe for 10 min. Lysates were centrifuged at 10,000 *g* for 10 min at 4°C and the supernatants were carefully transferred to new tubes for further steps.

Protein Digestion and iTRAQ Labeling

The protein concentration was determined by the Qubit Protein Assay Kit® fluorometric (Invitrogen), following the manufacturer's instructions. A total of 100 μg of proteins from each condition was processed. Protein samples were incubated with dithiothreitol (DTT; GE Healthcare) at 10 mM and 30°C for 1 h. Subsequently, iodoacetamide solution (GE Healthcare) was added, with a final concentration of 40 mM. The reaction was performed at room temperature, in the dark, for 30 min. The samples were diluted 10× with 50 mM HEPES buffer to reduce the concentration of urea/thiourea. The solution was incubated with trypsin (Promega) in a 1:50 (w/w, enzyme/protein) ratio at 37°C for 18 h. The resulting peptides were desalted with a C-18 macro spin column (Harvard Apparatus) and then vacuum dried. The dried peptides were labeled with isobaric tags for relative and absolute quantitation (iTRAQ) 4-plex (ABSciex). The labeling process was performed according to Murillo et al. (2017). Briefly, dried peptides were dissolved in 50 mM TEAB and iTRAQ tags were dissolved in dry ethanol, labeling was performed by mixing peptide and tag solutions for 1 h at room temperature. The four tag reactions were combined in a single tube (ratio 1:1:1:1) and dried in a speed vac prior to fractionation. Each condition was labeled as follows: (i) Tag 114 corresponds to sample W (*Wolbachia* infected); (ii) Tag 115 to sample A (none infection); (iii) Tag 116 to sample WZ (*Wolbachia* and ZIKV co-infection); and (iv) Tag 117 to sample Z (ZIKV infection).

Fractionation by Hydrophilic Interaction Chromatography and LC-MS/MS Analysis

The iTRAQ labeled peptide mixture was fractionated off-line by HILIC (hydrophilic interaction liquid chromatography) before LC-MS/MS analysis. The dried samples were resuspended in acetonitrile (ACN) 90% / trifluoroacetic acid (TFA) 0.1% and injected into Shimadzu UFLC chromatography using a TSKGel Amide-80 column (15 cm × 2 mm i.d. × 3 μm – Supelco), flow rate 0.2 ml/min; mobile phases A (ACN 85%/TFA 0.1%) and B (TFA 0.1%); gradient: 0% of phase B in 5 min; 0–10% of phase B from 5 to 10 min; 10–20% of phase B from 10 to 55 min; 20–100% of phase B from 55 to 60 min; and 100–0% of phase B from 60 to 65 min. For each pooled sample, eight fractions were collected and combined according to the separation and intensity of the peaks. The pools of fractions were dried in a speed vac and resuspend in 0.1% formic acid (FA). The samples were analyzed in Easy-nLC 1000 coupled to a Q-Exactive Plus mass spectrometer (Thermo Fisher Scientific). For each fraction (or pool of fractions), a linear gradient of 5–40% of B em 105 min, 40–95% in 8 min and 95% B in 5 min was performed in 120 min; phase A (0.1% FA), B (ACN 95%, 0.1% FA). Ionization was performed in an electrospray source with the acquisition of spectra in positive polarity by data-dependent acquisition (DDA) mode, spray voltage of 2.5 kV, and temperature of 200°C in the heated capillary. The acquisition was set as follows: full scan or MS1 in the range of 375–1,800 m/z, resolution of 70,000 (m/z 200), fragmentation of the 10 most intense ions in the HCD collision cell, with standardized collision energy (NCE) of 30, resolution of 17,000 in the acquisition of MS/MS spectra, the first mass of 110 m/z, isolation window of 2.0 m/z and dynamic exclusion of 45 s.

Data Analysis

The raw data were processed using Proteome Discoverer 2.4 Software (Thermo Fisher Scientific). Peptide identification was performed with the Sequest HT search engine against *A. aegypti* (genome version/assembly ID: INSDC: GCA_002204515.1), ZIKV, and *Wolbachia* databases provided by VectorBase (Giraldo-Calderón et al., 2015), ViPR (Pickett et al., 2012), and UniProt (The Uniprot Consortium, 2019), respectively. Searches were performed with peptide mass tolerance of 10 ppm, MS/MS tolerance of 0.1 Da, tryptic cleavage specificity, two maximum missed cleavage sites allowed, fixed modification of carbamidomethyl (Cys), variable modification of iTRAQ 4-plex (Tyr, Lys, and peptide N-terminus), phosphate (Ser, Thr, and Tyr), and oxidation (Met); peptides with high confidence were considered. False discovery rates (FDR) were obtained using Target Decoy PSM selecting identifications with a q-value equal or to less than 0.01. Data of all technical replicates were log2-transformed and normalized by subtracting the column median. Relative iTRAQ quantification analysis was carried out in the Perseus software, version 1.6.12.0 (Tyanova et al., 2016), based on the intensity of the fragmented reporter peaks in MS/MS.

Statistics and Gene Enrichment

For ZIKV peptides abundance comparison, statistical analysis was performed in experimental groups using T-test analysis (95% confidence values, $p < 0.05$), meanwhile for differential proteins was used one-way analysis of variance (ANOVA) and Tukey's multiple comparisons post-test (95% confidence values, $p < 0.05$) in Graphpad Prism 8.0.0 for Windows, GraphPad Software, San Diego, CA, United States, www.graphpad.com. Biological processes enrichment for differentially expressed proteins were performed using Fisher's Exact Test ($p < 0.05$) in VectorBase website (bit.ly/38OmEX0) (Ashburner et al., 2000; Giraldo-Calderón et al., 2015). The resulting Gene Ontology (GO) lists were summarized and represented in a network interaction format in REVIGO (Supek et al., 2011).

RESULTS AND DISCUSSION

Proteome Analysis

Proteomics has improved in recent years, especially considering its coverage and sensitivity, which offer more opportunities to study changes in the global proteome of complex tissues (Aebersold and Mann, 2016). Therefore, the use of isobaric-labeled quantitative proteomics measurements provides efficiency and increased depth coverage of proteomics analysis (Rauniyar and Yates, 2014). Peptides from the four experimental groups were labeled with iTRAQ 4-plex, enabling multiplexing of samples prior to off-line fractionation and LC-MS/MS analysis (**Figure 1**). We were able to identify 4,117 protein groups (**Table 1**), 26,898 peptides and 909,046 MS/MS spectra. The protein search was performed using *A. aegypti*, ZIKV, and *Wolbachia* databases simultaneously. Of all identified proteins, 3,790 belong to *A. aegypti*, 323 to *Wolbachia* and three unique peptides with a total of 10 PSMs to the ZIKV polyprotein (**Figure 2** and **Supplementary Figures 1**, **2**).

Quantitative Proteomics

The quantitative proteomics analysis was performed by comparing the four experimental groups using the normalized iTRAQ reporter ion intensity of identified peptides. Replicates were highly correlated (Pearson correlation mean of 0.97) and normalization methods were applied (**Supplementary Figure 3**). The 196 proteins with significant differences were statistically determined by the ANOVA test. Using the Tukey post-test ANOVA, we defined pairs of proteins with significant differences between the groups (**Supplementary Table 2**). The comparisons between the samples were: single-infected mosquitoes versus non-infected mosquitoes (W versus A and Z versus A); coinfected versus non-infected mosquitoes (WZ versus A); coinfected versus single-infected mosquitoes (WZ versus W and WZ versus Z).

Abundance of ZIKV Polyprotein Is Reduced in the Presence of *Wolbachia*

The quantitative analysis using the iTRAQ reporter ions from ZIKV peptides revealed that ZIKV proteins were more abundant in the absence of *Wolbachia* in contrast to mosquitoes coinfected

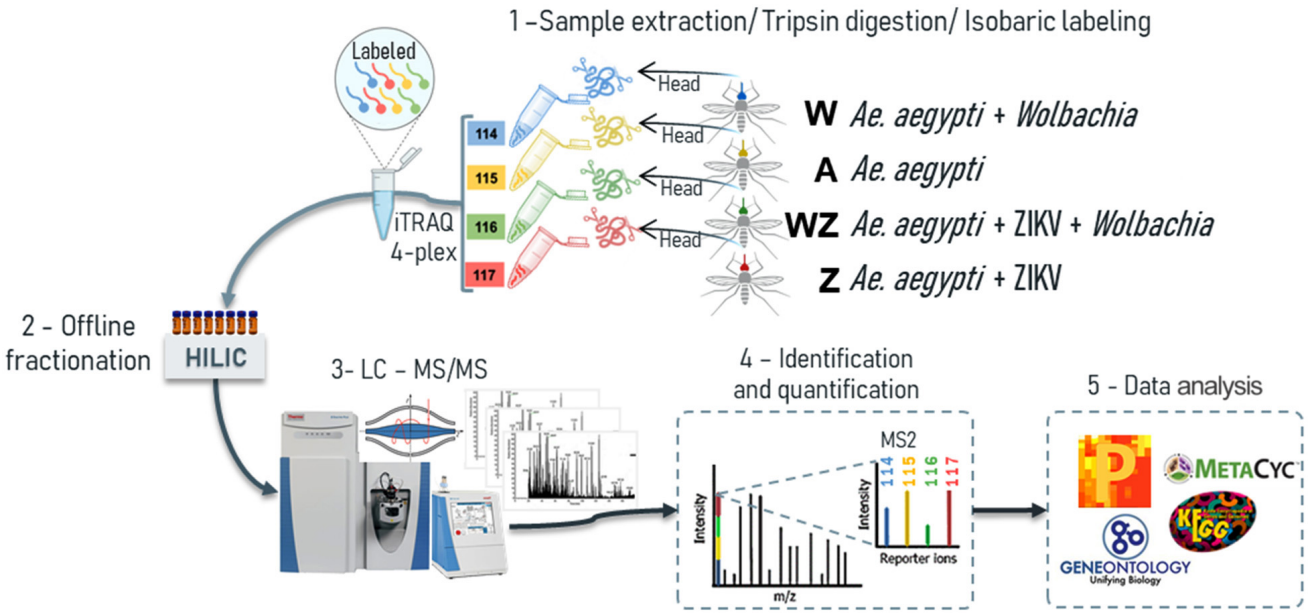

FIGURE 1 | The proteomics workflow carried out in the head + salivary gland of *A. aegypti* females used samples from four different conditions: A, non-infected mosquitoes; W, *Wolbachia* infected; Z, ZIKV infected; and WZ, *Wolbachia* and ZIKV infection. **1** – The samples were subjected to lysis and, subsequently, proteins were reduced, alkylated, and digested using trypsin. The resulting peptides were labeled with iTRAQ-4plex and combined in 1:1:1:1 ratio; **2** – labeled peptides were fractionated offline using HILIC chromatography; **3** – pool of fractions were analyzed by nLC–MS/MS in Q-Exactive Plus mass spectrometer; **4** – fragmentation of the attached tag release a low *m/z* reporter ions used for relative quantification of the peptides/proteins from which they originated; **5** – statistical analysis were performed in Perseus and bioinformatics analysis used Gene Ontology (GO) in the enrichment of proteins differentially regulated.

with ZIKV and *Wolbachia* (**Figure 2**). This latter condition showed reporter ions intensity compared to the background signal of uninfected mosquitoes (**Figure 2A**). This result indicates *Wolbachia* presence likely reduces virus replication in the female head and salivary gland (**Figure 2B**). Noteworthy, the presence of the *w*Mel strain in organs like salivary glands and ovaries of *A. aegypti* females induce the antiviral response that supports *Wolbachia* deployment to mitigate disease transmission.

The detection of ZIKV in the mosquito head + salivary gland was possible even considering that virus proteins were a minute fraction of all proteins identified. Peptides LITANPVITESTENS, SHTLWTDGIEESDLIIP, and LNQMSALEFYSYKK showed a robust increase in ZIKV infected tissue and this data represents a resource to further develop targeted proteomics methods to quantify ZIKV in infected mosquitoes (MS/MS spectra shown in **Supplementary Figure 1**).

Identification of Salivary Gland Proteins, Neuropeptides, and Hormones in Head Samples

During a blood meal, the female mosquitoes inject saliva into the host skin. The salivary glands produce a huge amount of molecules to avoid host responses against blood loss and to evade the host immune system (Ribeiro et al., 2016). For transmission of arboviroses, the virus must be secreted with the saliva during a blood meal in a vertebrate host (Linthicum et al., 1996). In this work, we took advantage of the sensitivity of protein detection by MS to detect and quantify proteins from the salivary gland, which are located on the anterior part of the thorax of *A. aegypti*. We compared the head proteome with two proteomes and one transcriptome (Wasinpiyamongkol et al., 2010; Ribeiro et al., 2016; Dhawan et al., 2017) from salivary glands of female mosquitoes to identify the salivary gland related proteins (**Figure 3**). We observed that among the 3,790 proteins identified in *A. aegypti* heads, 830 proteins were previously known to be expressed in the salivary glands. Moreover, we identified 77% of the proteins described by Wasinpiyamongkol et al. (2010) and 65% by Dhawan et al. (2017) in previous salivary gland proteome analysis. The 16 salivary proteins that were detected in all datasets probably are the most expressed and include inhibitors of platelet aggregation (salivary apyrase, AAEL006333-PA; apyrase precursor, AAEL006347PA), clotting inhibitors (SRPN23, AAEL002704-PB; SRPN26, AAEL003182-PA), aegyptins (AAEL010228-PA and AAEL010235-PA), angiopoietins (AAEL000749-PA and AAEL000726-PA), D7 family proteins (AAEL006417-PA and AAEL006424-PA), among others. We compared the 830 proteins previously known to be expressed in the salivary glands with the 196 differentially expressed proteins, to understand if these proteins could play a role during ZIKV and *Wolbachia* infections and/or co-infections. The modulation of saliva proteins is discussed below where the systemic changes in W, Z, and WZ will be addressed.

As a class of neuronal signal molecules, neuropeptides are produced by the neurosecretory cells, that are mainly located in the brain, suboesophageal ganglion, among others (Li et al., 2020). In insects, neuropeptides and their

TABLE 1 | Proteins with significative diferencial expression by ANOVA test ($p < 0.05$) and each respective pair analyzed by Tukey test.

Significant pairs (up-regulated_down-regulated)	Protein	(−Log ANOVA *P*-value)
A_Z;WZ_Z;A_W;WZ_W	AAEL026217-PA	4,271777813
WZ_Z;WZ_W;WZ_A	AAEL005656-PB myosin heavy chain, non-muscle or smooth muscle	2,514001451
WZ_W;WZ_A	AAEL009955-PB	2,195629072
A_W	AAEL001928-PA Act1: Actin-1	1,800850488
Z_WZ;W_WZ;A_WZ;W_Z;A_Z;A_W	AAEL012062-PX Na+/K+ ATPase alpha subunit	7,11879894
WZ_Z;A_Z	AAEL002565-PD titin	1,806231463
A_W	AAEL010975-PB paramyosin, long form	1,314499523
Z_W;A_W;WZ_W;WZ_Z;WZ_A	AAEL012897-PA aconitase, mitochondrial	4,240561485
WZ_A	AAEL009847-PB microtubule-associated protein	1,77714195
WZ_W	AAEL002851-PA tubulin beta chain	1,552090751
WZ_W	AAEL005422-PA pyrroline-5-carboxylate dehydrogenase	2,184255666
Z_W;WZ_W;Z_A;WZ_A	AAEL006138-PA	4,517435874
WZ_W;WZ_Z	AAEL002759-PD tropomyosin invertebrate	2,121497626
Z_W	AAEL011504-PA pupal cuticle protein, putative	1,607203142
WZ_W;A_W;WZ_Z;A_Z;A_WZ	AAEL006582-PH calcium-transporting ATPase sarcoplasmic/endoplasmic reticulum type	4,911628212
Z_W;A_W	AAEL002761-PAM tropomyosin invertebrate	1,677982154
A_W;WZ_W;Z_W;WZ_A;Z_A	AAEL006126-PA	4,511369267
WZ_Z;W_Z	AAEL001194-PA FAS1: fatty acid synthase	1,811428505
WZ_Z;A_Z;A_W	AAEL004297-PI ATP-citrate synthase	2,526180238
WZ_Z;WZ_W	AAEL012552-PA NADH-ubiquinone oxidoreductase	1,66727909
Z_W;WZ_W;Z_A;WZ_A	AAEL004988-PA Pgk: phosphoglycerate kinase	3,077106946
WZ_Z	AAEL006834-PA glutamate semialdehyde dehydrogenase	1,316789414
A_W	AAEL005798-PA ATP synthase subunit beta vacuolar	1,549407725
WZ_Z;WZ_A	AAEL013535-PA phosrestin ii (arrestin a) (arrestin 1)	2,17733154
Z_A;Z_W	AAEL015314-PM cAMP-dependent protein kinase type ii regulatory subunit	2,098280165
WZ_Z;A_Z;WZ_W;A_W	AAEL024235-PG	2,840685255
A_W	AAEL004423-PA mitochondrial F0 ATP synthase D chain, putative	1,402250531
A_Z;A_W	AAEL024583-PB	2,16614374
WZ_W;WZ_Z	AAEL017301-PA elongation factor 1-alpha	1,855121353
Z_W;WZ_W;A_W;WZ_Z;A_Z	AAEL012326-PA calmodulin	6,629410461
WZ_A;WZ_W;WZ_Z	AAEL010823-PA ATP synthase delta chain	2,406253156
WZ_Z;WZ_W;WZ_A	AAEL008542-PF kinesin heavy chain subunit	2,621489163
WZ_W;WZ_A	AAEL017096-PA elongation factor 1-alpha	1,635565462
WZ_W;WZ_A	AAEL017293-PA	2,296841727
Z_A;Z_W	AAEL008773-PA laminin A chain, putative	1,916965629
WZ_A;WZ_W	AAEL015458-PA Tf1: transferrin	2,50568231
WZ_Z;A_Z;A_W	AAEL000596-PB myosin	2,481800641
WZ_A;Z_A;Z_W;Z_WZ	AAEL013279-PB peptidyl-prolyl cis-trans isomerase (cyclophilin)	4,651840282
Z_W;WZ_W;WZ_A	AAEL011981-PA glutamate decarboxylase	3,261398284
Z_W;A_W;A_WZ	AAEL013952-PD prohibitin	2,15301324
WZ_W	AAEL010143-PA isocitrate dehydrogenase	1,974182672
WZ_W	AAEL005997-PA allergen, putative	1,313495456
WZ_W	AAEL012207-PF myosin light chain 1	1,319537308
WZ_A	AAEL001677-PA	1,609275972
WZ_W;WZ_Z	AAEL008844-PA calcium-binding protein, putative	2,040394666
W_A;WZ_A	AAEL004088-PH aldo-keto reductase	2,504453412
WZ_W;Z_W;A_W	AAEL011758-PA peptidyl-prolyl cis-trans isomerase f, ppif	2,772874519
W_A;WZ_A;W_Z;WZ_Z;WZ_W	AAEL014600-PA 4-hydroxyphenylpyruvate dioxygenase	5,467053042
Z_W;WZ_W	AAEL001082-PA	1,829540732
W_Z;W_WZ	AAEL004559-PJ synaptosomal associated protein	1,686140462
W_A;WZ_A	AAEL012827-PA endoplasmin	1,859306212
WZ_A;WZ_Z	AAEL001683-PA	2,403005778

(Continued)

TABLE 1 | Continued

Significant pairs (up-regulated_down-regulated)	Protein	(−Log ANOVA *P*-value)
WZ_W	AAEL001473-PC dynamin-associated protein	1,404560111
WZ_W;Z_W	AAEL007383-PE secreted ferritin G subunit precursor, putative	1,89879228
Z_W;A_W;WZ_W;WZ_Z;WZ_A	AAEL005407-PD annexin x	3,750898348
WZ_W;A_W;Z_W;A_WZ;Z_WZ;Z_A	AAEL008789-PA apolipophorin-III, putative	6,190366803
A_W	AAEL006946-PA chaperonin	1,282782467
WZ_A;Z_A;Z_W	AAEL011090-PA complement component	2,669480529
Z_A;WZ_A;WZ_W	AAEL009389-PA transaldolase	1,98264351
WZ_W;Z_W	AAEL023497-PA protein-L-isoaspartate O-methyltransferase	2,775892202
A_W;Z_W;WZ_W	AAEL004745-PA pupal cuticle protein, putative	2,586973455
Z_W;A_W;WZ_W;WZ_Z;WZ_A	AAEL019951-PG	4,789914023
WZ_A	AAEL000934-PI clathrin light chain	1,919802572
A_Z	AAEL004041-PD flotillin-2	1,321402995
Z_W;Z_WZ	AAEL013338-PA lethal(2)essential for life protein, l2efl	1,487090987
Z_A;WZ_A	AAEL010840-PB	2,229411597
Z_A;W_A;WZ_A;WZ_Z	AAEL001851-PB	4,012423993
WZ_A	AAEL004176-PB microtubule binding protein, putative	2,027657273
WZ_A	AAEL001794-PB macroglobulin/complement	1,757699803
A_W;Z_W;WZ_W	AAEL019778-PA	2,545595403
Z_WZ;Z_W	AAEL022352-PA	1,719161308
WZ_W	AAEL001946-PA four and a half lim domains	1,870893776
W_A;WZ_A;WZ_Z	AAEL017263-PA	2,835314331
WZ_W;Z_W	AAEL006271-PD CUSOD2: copper-zinc (Cu-Zn) superoxide dismutase	1,612285952
WZ_W	AAEL002185-PA cuticle protein, putative	2,210230165
Z_W;A_W;WZ_W	AAEL005946-PA NADH-ubiquinone oxidoreductase subunit B14.5b	3,524279291
A_Z	AAEL006948-PB tomosyn	1,630732328
WZ_W;A_W	AAEL006027-PB lipase	2,512978955
Z_WZ;W_WZ;Z_A;W_A	AAEL012206-PB microtubule-associated protein tau	3,461529529
W_A;WZ_A;Z_A	AAEL000762-PB LRIM19: leucine-rich immune protein (Coil-less)	2,533734366
Z_A;Z_W	AAEL013138-PA	2,190112627
WZ_Z;WZ_A	AAEL003888-PD ubiquitin	1,499108348
Z_WZ	AAEL014416-PC pupal cuticle protein 78E, putative	1,95874832
Z_A	AAEL025999-PA 40S ribosomal protein S17	1,533198334
WZ_W	AAEL009257-PA	1,735940859
W_A;Z_A;WZ_A;WZ_W;WZ_Z	AAEL017212-PA	4,19347108
WZ_A;WZ_Z;WZ_W	AAEL015424-PA adult cuticle protein, putative	2,324346555
A_W;WZ_W;A_Z;WZ_Z	AAEL009604-PG receptor expression-enhancing protein	2,983369006
A_WZ;W_WZ;Z_WZ;Z_A	AAEL018211-PB	4,186777407
WZ_W	AAEL010168-PA RpS2: 40S ribosomal protein S2	1,566481125
WZ_A	AAEL012865-PA	1,317062128
WZ_A	AAEL004148-PA heat shock protein 70 (hsp70)-interacting protein	1,394760066
W_WZ;Z_WZ	AAEL019767-PA	2,164853975
Z_W;A_W	AAEL019793-PB	1,761699228
Z_A	AAEL011982-PC cortactin	1,798033943
A_W	AAEL001864-PA eukaryotic translation initiation factor 4E binding protein (4EBP)	1,306963121
A_W	AAEL019718-PA	1,510324956
Z_A;Z_WZ	AAEL000028-PA CLIPB34: clip-domain serine protease family B.	1,708280762
W_WZ;A_WZ	AAEL007010-PA CYP6AG4: cytochrome P450	1,700443182
W_A	AAEL013808-PF fascin	1,388013685
WZ_A;WZ_Z	AAEL006406-PG Putative 14.5 kDa secreted protein	1,957996691
A_Z;A_W	AAEL009398-PA Pep12p, putative	1,979171968
A_W;A_Z	AAEL018664-PA COX2: cytochrome c oxidase subunit II	2,547584077
W_WZ;A_WZ	AAEL000090-PB secretory carrier-associated membrane protein (scamp)	2,674457264

(Continued)

TABLE 1 | Continued

Significant pairs (up-regulated_down-regulated)	Protein	(−Log ANOVA *P*-value)
W_WZ;W_Z	AAEL006719-PA AMY1: alpha-amylase I precursor (EC 3.2.1.1) (1,4-alpha-D-glucan glucanohydrolase)	1,919418688
WZ_W	AAEL006677-PA phospholipase a-2-activating protein	1,334478579
WZ_A;WZ_Z;WZ_W	AAEL003954-PA juvenile hormone-inducible protein, putative	2,79570589
WZ_A;Z_A;W_A	AAEL001402-PA LRIM10B: leucine-rich immune protein (Short)	2,43294121
WZ_A	AAEL003431-PA proteasome subunit beta type 7,10	1,308314374
W_WZ;Z_WZ;A_WZ;A_W;A_Z	AAEL005793-PA AMP dependent ligase	5,868868376
A_WZ;W_WZ;Z_WZ;Z_A;Z_W	AAEL009653-PA RpS30: 40S ribosomal protein S30	6,088741815
Z_A;W_A	AAEL008422-PD	1,806945766
A_Z;A_W;A_WZ	AAEL009314-PA adenylate cyclase	1,930417494
WZ_Z;W_Z;WZ_A;W_A	AAEL002245-PA	3,537852527
Z_A	AAEL001077-PA CLIPB45: clip-domain serine protease family B. Protease homologue.	1,565423585
A_WZ	AAEL004146-PA CRY1: cryptochrome 1	1,391490707
Z_WZ;A_WZ;A_W	AAEL003104-PC tripartite motif protein trim2,3	3,162779729
A_W;Z_W;A_WZ;Z_WZ	AAEL006124-PA mitochondrial import inner membrane translocase subunit TIM50	2,7915452
Z_W	AAEL006464-PA	1,348559818
Z_W;Z_WZ;Z_A	AAEL009642-PA cathepsin b	2,135923633
Z_WZ;Z_A	AAEL013119-PA charged multivesicular body protein	2,331529326
WZ_W;WZ_Z;WZ_A	AAEL014372-PA juvenile hormone-inducible protein, putative	2,942325794
Z_WZ;A_WZ;Z_W;A_W	AAEL008764-PA cuticle protein, putative	3,385118481
Z_A;WZ_A;W_A	AAEL010139-PA serine protease, putative	2,963764022
W_Z;W_WZ;W_A	AAEL014961-PA gdp mannose-4,6-dehydratase	2,125006815
A_W;A_Z;A_WZ	AAEL009863-PD sodium/dicarboxylate cotransporter, putative	3,502744434
Z_WZ;A_WZ;W_WZ	AAEL000556-PA CTL25: C-Type Lectin (CTL25)	2,692047592
W_A	AAEL010491-PB FKBP12: fk506-binding protein	1,445125001
Z_WZ;A_WZ;A_W;A_Z	AAEL003188-PA sphingosine phosphate lyase	3,331676114
W_A;W_WZ;W_Z	AAEL027103-PA	1,821833076
A_Z;A_WZ	AAEL006002-PA	2,106633723
W_WZ	AAEL005469-PB	2,324487859
WZ_W;A_W	AAEL006971-PA	1,967613183
A_WZ	AAEL020992-PE	1,369902298
W_Z;W_WZ	AAEL009974-PA ras-related protein Rab-8A, putative	1,757153294
W_A;WZ_A	AAEL009212-PG lola	1,512195091
WZ_W;Z_W	AAEL011070-PA CTLGA3: C-Type Lectin (CTL) – galactose binding.	2,201901256
A_W	AAEL018353-PB	1,570541993
Z_W;WZ_W;Z_A;WZ_A	AAEL008250-PC	2,137421729
W_WZ;W_A	AAEL008490-PC NADH dehydrogenase, putative	2,234786037
WZ_W;A_W;WZ_Z;A_Z;A_WZ	AAEL026670-PA	5,34600802
W_A	AAEL002135-PA tubulin-specific chaperone b (tubulin folding cofactor b)	1,71317976
A_W;A_Z	AAEL002350-PA	2,070802008
WZ_W;Z_W;A_W;A_WZ	AAEL011388-PA Vacuolar-sorting protein SNF8	6,982654776
W_WZ;A_WZ	AAEL002317-PE InR: Insulin-like receptor Precursor (MIR) (EC 2.7.10.1)	2,088114025
W_A;Z_A;WZ_A;WZ_W;WZ_Z	AAEL010059-PA bacterial-type ABC transport ATP-binding subunit? or RNAse l inhibitor	3,507872757
A_W;A_Z;A_WZ	AAEL022886-PA	2,240673165
W_A	AAEL015430-PB CLIPB19: clip-domain serine protease family B. Protease homologue.	2,153234226
Z_WZ	AAEL011433-PA small nuclear ribonucleoprotein sm d3	1,310683895
Z_W;WZ_W;A_W	AAEL019654-PB	2,186666781
Z_W;A_W;Z_WZ;A_WZ	AAEL015180-PB smooth muscle caldesmon, putative	2,511924586
A_WZ	AAEL003059-PB	1,594979945
W_Z	AAEL010408-PD GPRGBB2: GPCR GABA B Family	1,416228099

(Continued)

TABLE 1 | Continued

Significant pairs (up-regulated_down-regulated)	Protein	(−Log ANOVA *P*-value)
W_WZ;Z_WZ	AAEL006451-PB	1,791040044
W_WZ;Z_WZ;A_WZ;A_W	AAEL022232-PA	3,004180084
WZ_A;WZ_Z;WZ_W	AAEL014325-PA proteasome regulatory subunits	1,833896368
WZ_A	AAEL009833-PA mRpL46: mitochondrial ribosomal protein, L46, putative	1,348750399
Z_WZ;A_WZ;A_W	AAEL021103-PA	2,295144608
Z_WZ;W_WZ;A_WZ	AAEL011234-PC reticulon/nogo receptor	2,780134195
W_Z;W_A;W_WZ	AAEL010681-PA sodium/chloride dependent neurotransmitter transporter	2,743872823
Z_A;W_A;Z_WZ;W_WZ	AAEL008458-PA	3,128904889
WZ_A;Z_A;W_A;Z_WZ;W_WZ	AAEL007805-PA	3,307690677
W_A;Z_A;W_WZ;Z_WZ	AAEL002591-PA OBP13: odorant binding protein OBP13	3,101064427
WZ_W;A_W;Z_W;A_WZ;Z_WZ	AAEL019579-PA	3,390568158
W_WZ;Z_WZ	AAEL007821-PA signalosome, subunit 2, CSN8, putative	2,05489339
Z_WZ;A_WZ;W_WZ;W_Z;W_A	AAEL007420-PB SRPN25: serine protease inhibitor (serpin) homologue – unlikely to be inhibitory	3,948336385
WZ_W;A_W;WZ_Z;A_Z	AAEL019517-PA	2,852828682
WZ_Z;W_Z;WZ_A;W_A	AAEL002915-PA	1,982345339
W_Z;W_A;W_WZ	AAEL009589-PA	1,809032341
WZ_Z;WZ_A	AAEL009375-PK plekhh1	1,648776888
W_A	AAEL009951-PA dimeric dihydrodiol dehydrogenase	1,395167766
Z_WZ	AAEL014511-PE	1,422163284
Z_A;WZ_A;WZ_W;WZ_Z	AAEL029038-PA CECA: cecropin	4,563490639
Z_A;WZ_A;W_A;W_Z;W_WZ	AAEL002601-PA CLIPA1: clip-domain serine protease family A. Protease homologue.	2,487458073
Z_A;W_A;WZ_A	AAEL024070-PA putative small nuclear ribonucleoprotein snrnp smf	2,10243834
Z_WZ	AAEL000937-PA	1,954272132
A_WZ;Z_WZ;W_WZ	AAEL000330-PA	1,700894246
Z_WZ;A_WZ;W_WZ	AAEL005944-PA mRpS23: mitochondrial ribosomal protein, S23, putative	1,850199634
Z_A;W_A;W_WZ	AAEL018131-PB	2,234278377
WZ_Z;W_Z;A_Z	AAEL003991-PH alcohol dehydrogenase	2,241277965
Z_A;WZ_A;W_A	AAEL020192-PA	2,866821279
Z_WZ;Z_A;Z_W	AAEL021230-PA	2,059537005
Z_A;WZ_A;W_A;WZ_Z;W_Z	AAEL009026-PD ubiquitin-conjugating enzyme m	3,465385818
A_W	AAEL004300-PB	1,683474263
A_WZ	AAEL001950-PB	1,355021154
W_A;Z_A;Z_WZ	AAEL023091-PA	2,133515319
W_Z;W_WZ;W_A	AAEL013989-PA protein translocation complex beta subunit, putative	2,973482988
W_A	AAEL004406-PD	1,397828331
A_Z	AAEL012841-PA	1,589217982
A_W;Z_W;WZ_W;WZ_A;WZ_Z	AAEL011216-PG phosphatidylinositol-4,5-bisphosphate 4-phosphatase	3,386553816
Z_A;W_A;WZ_A	AAEL002102-PB	2,230950028
WZ_A;Z_A;W_A;Z_WZ;W_WZ;W_Z	AAEL018117-PB	3,946110261
Z_W;WZ_W;A_W	AAEL010791-PA Autophagy-specific protein, putative	3,986947222
W_Z;W_WZ;W_A	AAEL014516-PA metalloproteinase, putative	3,17627519
Z_W;A_W;A_WZ	AAEL011890-PC	2,288170865
W_Z;A_Z;W_WZ;A_WZ	AAEL008557-PA	2,838859624

receptors play important physiological processes such as development, reproduction, behavior, and feeding (Holt et al., 2002). A previous study that investigated the presence of neuropeptidomics in *A. aegypti* proteome carried out in the central nervous system (CNS) and midgut samples identified 43 neuropeptides and hormones (Predel et al., 2010). Of these, we were able to identify 13 in our head proteomics analysis (**Figure 4**): pyrokinin (PK) (AAEL012060), short

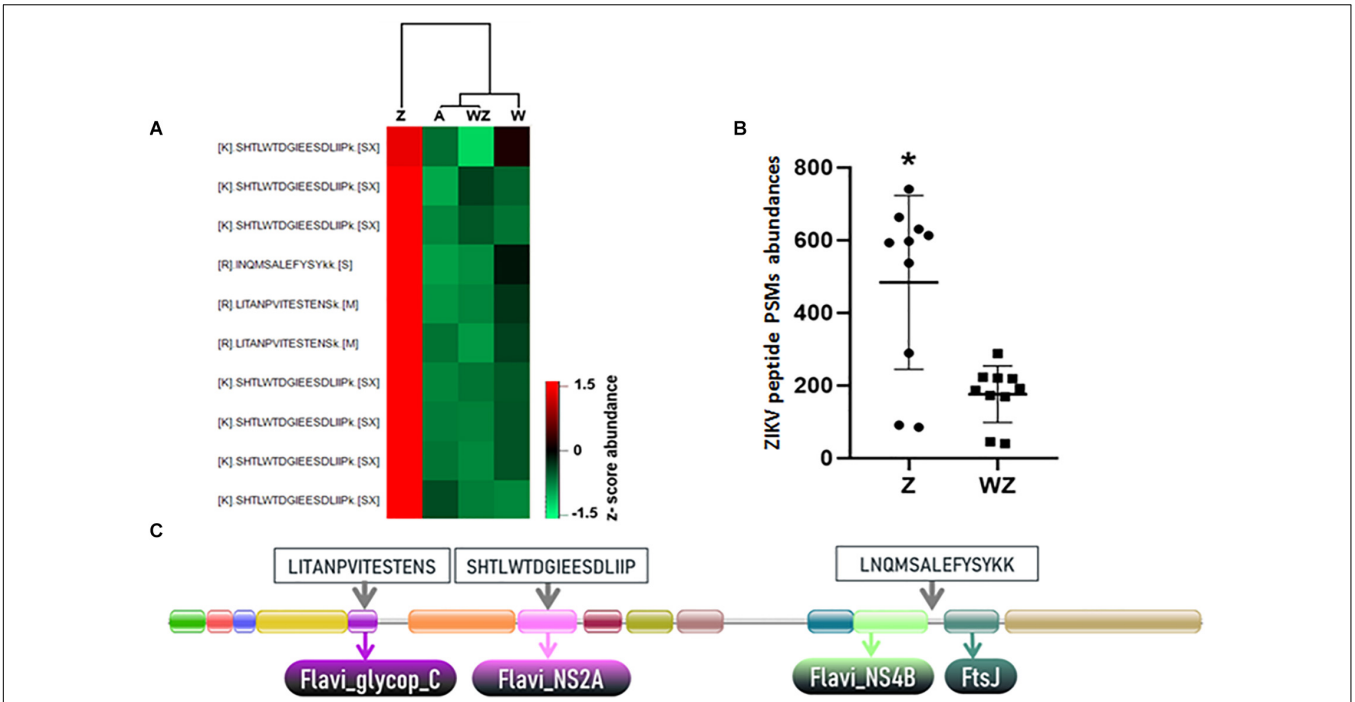

FIGURE 2 | Identification and quantification of ZIKV peptides. **(A)** Heatmap of ZIKV PSMs identified in the *A. aegypti* head + salivary gland generated in Perseus software using abundance values transformed by *z*-score. **(B)** Total abundance of peptides spectrum matches (PSMs) calculated from report ions intensities from the three ZIKV peptides identified in samples. "*" Means that in Statistical analysis (*T*-test; **P*-value 0.0011), developed by using the software GraphPad Prism 7.0, sample Z has a statistical difference to sample WZ. **(C)** Domain architecture of the complete ZIKV polyprotein obtained from the PFAM database (PF01570) (El-Gebali et al., 2018). The location within the conserved domains and amino acid sequence of the three unique ZIKV peptides identified in proteomics analysis are highlighted.

neuropeptide F (sNPF) (AAEL019691), neuropeptide-like precursor-1(NPLP) (AAEL012640), calcitonin-like diuretic hormone (DH-31) (AAEL008070), SIFamide (AAEL009858), crustacean cardioactive peptide (CCAP) (AAEL000630), allatotropin (AAEL009541), CAPA (AAEL005444), sulfakinin (SK) (AAEL006451), ovary ecdysteroidogenic hormone (OEH; neuroparsin A homolog) (AAEL004155), insulin-like peptide 1 and 7 (AAEL000937; AAEL024251), and adipokinetic hormone 1 (AKH) (AAEL011996). A few neuropeptides and hormones were modulated by co-infection and will be discussed afterward.

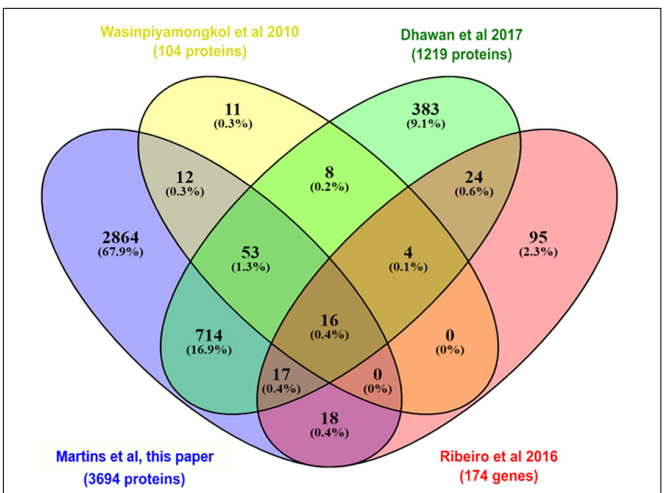

FIGURE 3 | Venn diagram comparing the set of proteins (isoforms were not considered) identified in this work (purple) with two previous proteomes of the salivary glands of *A. aegypti* (yellow; Wasinpiyamongkol et al., 2010 and green; Dhawan et al., 2017) and one transcriptome (red; Ribeiro et al., 2016) also carried out in salivary glands of *A. aegypti*, but in non-infected females.

ZIKV Infection Modulates Aerobic Metabolism, Lipids Pathways, and Immune System Response

By comparing mosquitoes infected and non-infected with ZIKV (**Figure 5** and **Supplementary Figure 4A**), we observe four main enriched processes: nicotinamide nucleotide metabolism, lipid transport, humoral innate response, and carbohydrate catabolism. Nicotinamide mononucleotide (NMN) is known for being an intermediator in NAD+ biosynthesis (Poddar et al., 2019; Hong et al., 2020), which participates actively in the aerobic metabolism process. This enrichment is mediated by the phosphoglycerate kinase (AAEL004988) and transaldolase (AAEL009389) upregulation, leading to carbohydrate catabolism elevation. The pentose phosphate pathway (PPP) was also up-regulated in our study as a response to transaldolase (AAEL009389) protein. The PPP is known to generate NADPH and pentoses (5-carbon sugars) as well as ribose 5-phosphate, a precursor for the synthesis of nucleotides, this led us

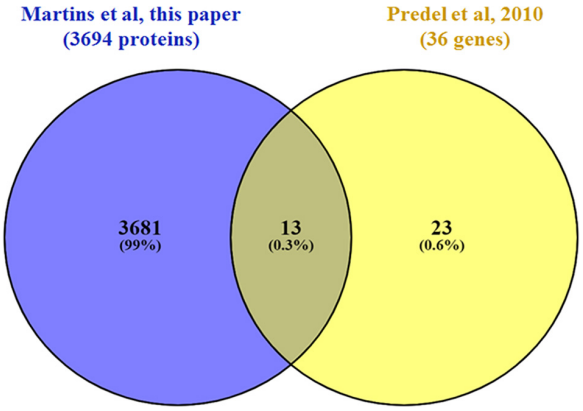

FIGURE 4 | Venn diagram comparing the set of neuropeptides and hormones (isoforms were not considered) identified in this work (purple) with those identified in Predel (yellow; Predel et al., 2010).

to relate the activation of PPP with the probation of nucleotide biosynthesis for virus replication (Guo et al., 2019). Both increased fluxes have been observed following Human Cytomegalovirus, Mayaro, and Kaposi-sarcoma viruses in human cells (El-Bacha and Da Poian, 2013).

Viruses are capable of modulating mitochondrial bioenergetics aiming to synthesize macromolecular precursors for self-replication, assembly and egress (El-Bacha and Da Poian, 2013). Thus, the enhancement of the lipid transport process should drive a redirection of these energetic resources to the viral capsids formation (Kuzmina et al., 2020), an event that was also described in *A. aegypti* coinfected with DENV and *Wolbachia* (Koh et al., 2020). Koh et al. (2020) compared lipid abundances between non-infected and DENV-3 infected mosquitoes and found that most modulated lipids are glycerophospholipids, as described earlier (Perera et al., 2012), with a higher level of unsaturated fatty acids and triacylglycerols. Glycerophospholipids modulation can be related to a virus attempt to build new virus capsids, as these lipids are a compound of this structure (Martín-Acebes et al., 2016). In our results, three genes related to lipid localization and transport were up-regulated: apolipophorin-III (AAEL008789) and two vitellogenin-A1 precursors (AAEL006126 and AAEL006138). Apolipophorins are protein components of lipoprotein particles that are essential for lipid transportation in the insect body, but apolipophorin-III can work as a pattern recognition receptor for insect immune system response (Wang et al., 2019), including in *A. aegypti* (Phillips and Clark, 2017). Lipid carrier protein lipophorin (Lp) and its lipophorin receptor (LpRfb) were significantly increased in *A. aegypti* after infections with Gram (+) bacteria and fungi, suggest that lipid metabolism is involved in the mosquito systemic immune responses to pathogens and parasites, as seen in studies before using fat body tissue (Cheon et al., 2006). The apolipophorin-III upregulation can be rolled to lipid transport and also to the immune response as ZIKV is expected to regulate them and the protein participates in both processes.

Another group of up-regulated biological processes includes an innate immune response in host cells due to virus infection (antimicrobial humoral response, humoral immune response, and response to biotic stimulus). Xi et al. (2008) found a significant role for the Toll pathway in DENV resistance regulation, and it was possible to identify differentially expressed antimicrobial peptide cecropin (AAEL029038) related to this pathway in our samples, confirming that Toll-pathway plays a major part in virus response (Xi et al., 2008; Pan et al., 2012; Kingsolver et al., 2013).

We observed down-regulation of tomosyn (AAEL006948), adenylate cyclase (AAEL009314), putative syntaxin-7 (AAEL009398), putative sodium/dicarboxylate cotransporter (AAEL009863), cytochrome c oxidase subunit II (AAEL018664), major facilitator superfamily domain-containing protein (AAEL006002), nuclear pore complex protein Nup188 (AAEL008557). and talin-1 (AAEL024235) related to cation transport processes. Also, three proteins were down-regulated: calcium-transporting ATPase sarcoplasmic/endoplasmic reticulum type (AAEL006582), Na+/K+ ATPase alpha subunit (AAEL012062), and calmodulin (AAEL012326-PA) related to cation transport processes as well. Similarly cytoskeleton, vesicle-mediated transport and ion transport-associated proteins down-regulation were described in CHIKV infection (Cui et al., 2020). Also, a recent study showed that Na+/K+ ATPase inhibition using two distinct drugs in mice helped to block ZIKV replication (Guo et al., 2020), suggesting that this down-regulation could be a mosquito cellular response to fight infection.

Adenosine triphosphate-citrate synthase (AAEL004297), sphingosine phosphate lyase (AAEL003188) and probable cysteine-tRNA synthetase (AAEL022886), proteins associated with amino acids insertion in the citric acid cycle, were also down-regulated and may lead to a decrease in citric acid cycle and oxidative phosphorylation processes. This phenomenon was also observed in *A. aegypti* salivary glands infected with DENV-2 (Chisenhall et al., 2014; Shrinet et al., 2018), suggesting the occurrence of cellular biomolecule and energy production control by virus infection to avoid mitochondrial exhaustion.

Wolbachia Endosymbiosis Interfere in Glycoconjugates Production Pathways, Aerobic Metabolism, Immune Response Induction, and Blood-Feeding Process

It is possible to notice in our data (**Figure 6** and **Supplementary Figures 3B, 4B**) an enrichment of GDP-mannose metabolism comparing mosquitoes non-infected with *Wolbachia*-mono infected. The enrichment was based on the upregulation of gdp mannose-4,6-dehydratase (AAEL014961), which converts GDP-mannose to GDP-4-dehydro-6-deoxy-D-mannose, the first of three steps for the conversion of GDP-mannose to GDP-fucose. This result suggests an induction caused by the presence of *Wolbachia* in insect cells to generate glycoconjugates, as GDP-mannose is a precursor for these molecules (Stick and Williams, 2009; Rexer et al., 2020), that may be used as elements to form new bacterial structures (García-del Portillo, 2020). An important

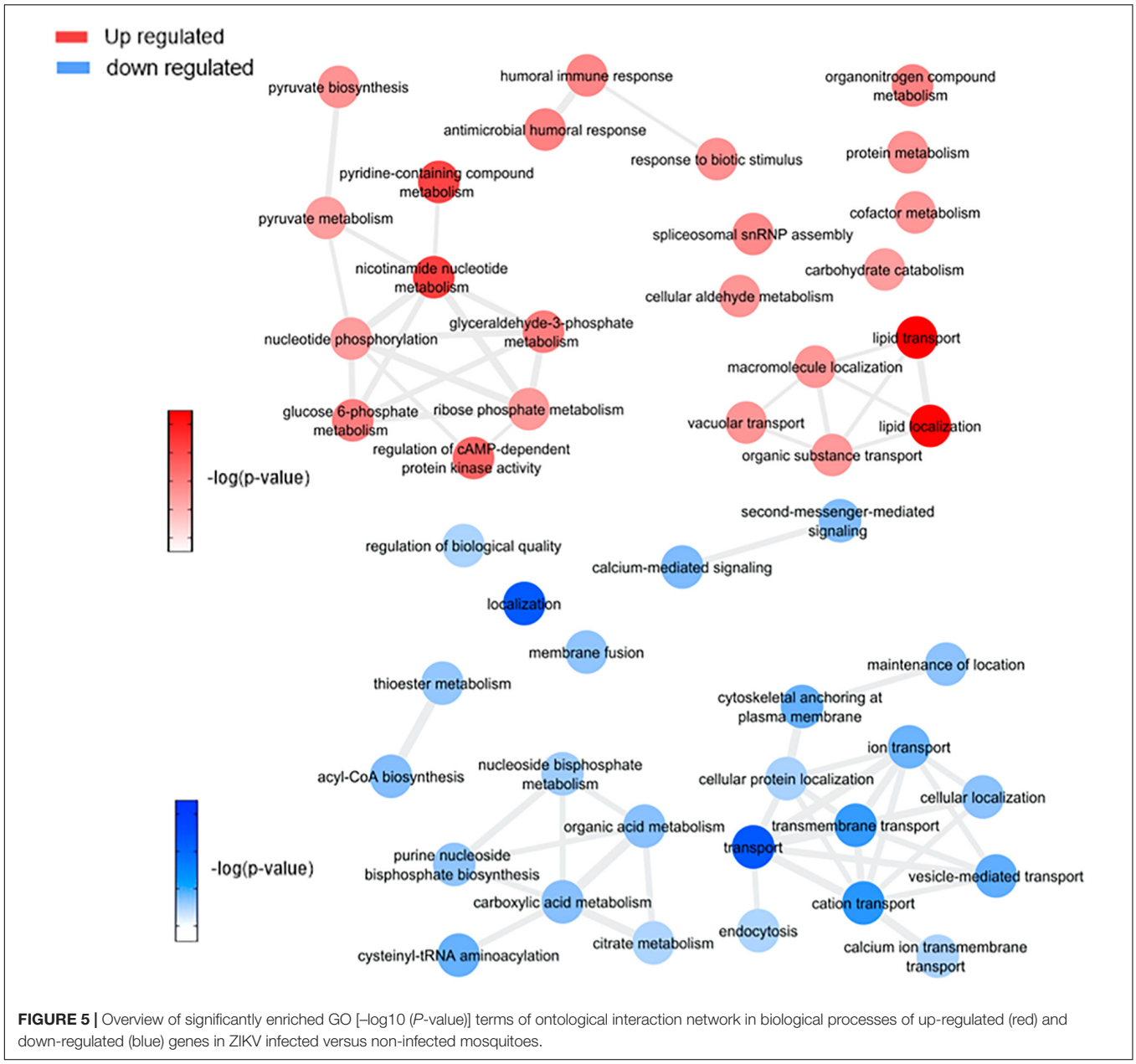

FIGURE 5 | Overview of significantly enriched GO [–log10 (*P*-value)] terms of ontological interaction network in biological processes of up-regulated (red) and down-regulated (blue) genes in ZIKV infected versus non-infected mosquitoes.

observation was the enrichment of processes downregulated related to the citric acid cycle in mosquito cells infected with *Wolbachia*. As shown by da Rocha Fernandes et al. (2014), *Wolbachia* modulated glycogen metabolism in *Aedes fluviatilis* embryos in favor of its aerobic metabolism (da Rocha Fernandes et al., 2014).

Up-regulation of 4-hydroxyphenylpyruvate dioxygenase (AAEL014600) can be related to plastoquinol and vitamin E (tocopherol) synthesis. Both molecules are described in the literature as participants of antioxidant response to different stimuli in organisms (MaitiDutta et al., 2020; Nowicka et al., 2020), including oxidative stress (Kumar et al., 2020; Minter et al., 2020). In this way, we consider that genes correlated to these pathways were regulated during *Wolbachia* infection because this microorganism can induce the expression of antioxidant proteins (Brennan et al., 2008). Moreover, 4-hydroxyphenylpyruvate dioxygenase is related to L-tyrosine degradation I and L-phenylalanine degradation IV, which are essential traits for blood-feeding arthropods, as they consume an amount of blood proteins and need to deal with a high quantity of free amino acids (Sterkel et al., 2016).

The *Wolbachia* infection up-regulated 10 salivary gland proteins, such as endoplasmin (AAEL012827-PA), which is required for proper folding of Toll-like receptors in mammals (Fitzgerald and Kagan, 2020), and FKBP12 (AAEL010491-PB) that has a prolyl isomerase activity and bidins to immunosuppressive molecules (Caminati and Procacci, 2020).

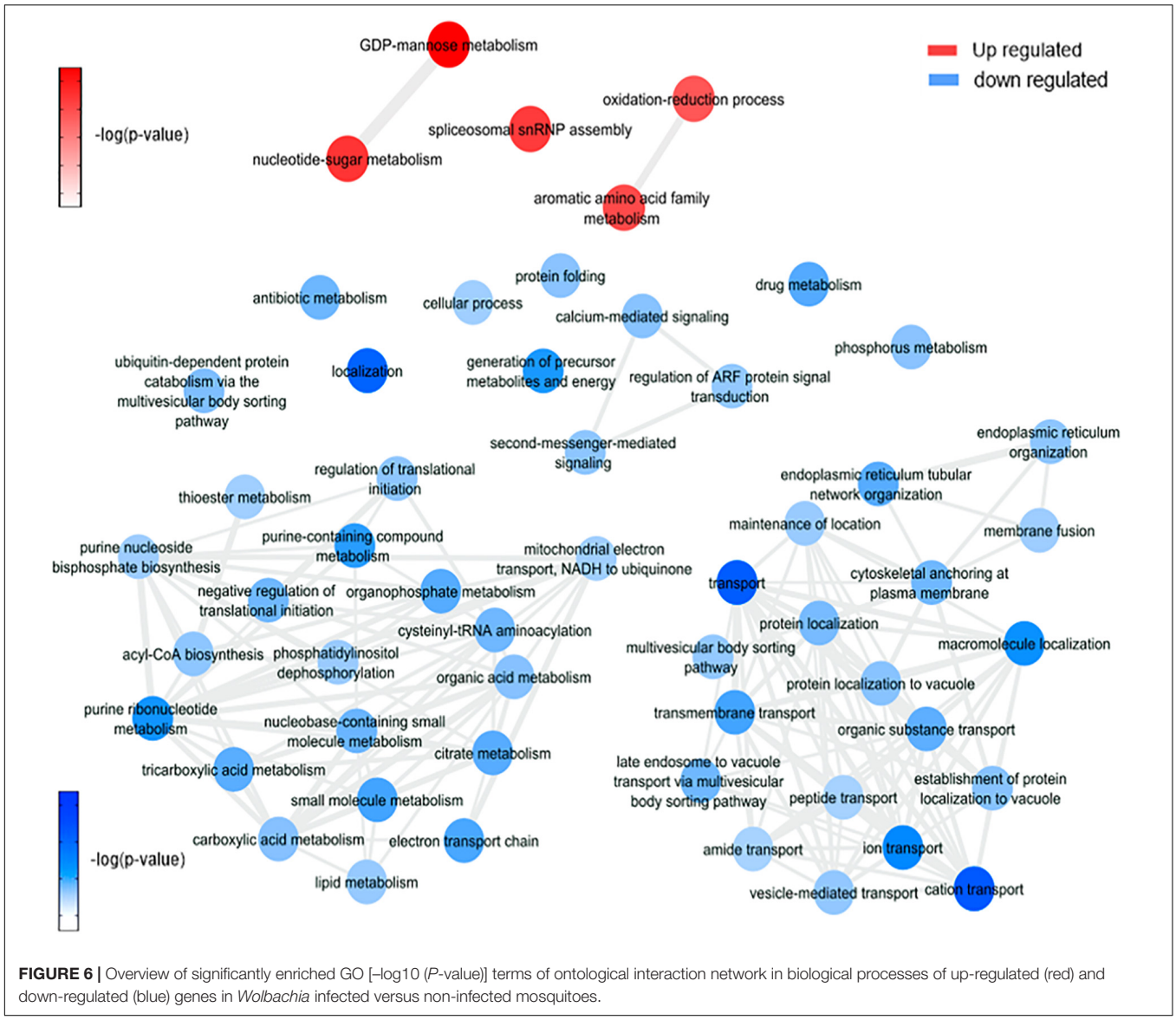

FIGURE 6 | Overview of significantly enriched GO [–log10 (*P*-value)] terms of ontological interaction network in biological processes of up-regulated (red) and down-regulated (blue) genes in *Wolbachia* infected versus non-infected mosquitoes.

Twenty salivary proteins were down-regulated by *Wolbachia* infection. Interestingly, the same ion related proteins down-regulated by ZIKV are also down-regulated by *Wolbachia*, moreover, proteins related with contraction such as paramyosin (AAEL010975-PA), tropomyosin (AAEL002761-PA), and Actin-1 (AAEL001928-PA) were also down-regulated. Also, a serine protease inhibitor 25 (SRPN25) (AAEL007420-PB) was also identified in our analysis. Its orthologue is Alboserpin, the major salivary gland anticoagulant in *Aedes albopictus*, which prevents coagulation in an atypical reversible interaction with factor Xa (coagulation activation factor), important for blood intake by female mosquitoes (Stark and James, 1998; Calvo et al., 2011). SRPN25 was up-regulated in W, which may infer that blood takes longer to coagulate, increasing mosquito enzymes access to digest blood. The consequence of these salivary proteins modulation suggests an impairment in salivary gland injection into the host and a possible reduction in the amount of blood ingestion during *Wolbachia* presence in the mosquito (Turley et al., 2009).

Co-infection Modulated Pathways and Processes Show an Induction in Reactive Oxygen Species Production That Can Lead to an Immune System Response to Virus Infection

This analysis was based on a comparison of the ZW with Z (**Figure 7** and **Supplementary Figure 4C**) and W (**Figure 8** and **Supplementary Figure 4D**) mosquito heads samples.

Zika virus and *Wolbachia* use mosquitoes cell machinery respectively to synthesize lipids and glycoconjugates molecules for their structural use, as mentioned before. According to WZ results, the enriched lipid synthesis biological processes remain up-regulated despite the *Wolbachia* presence, similarly

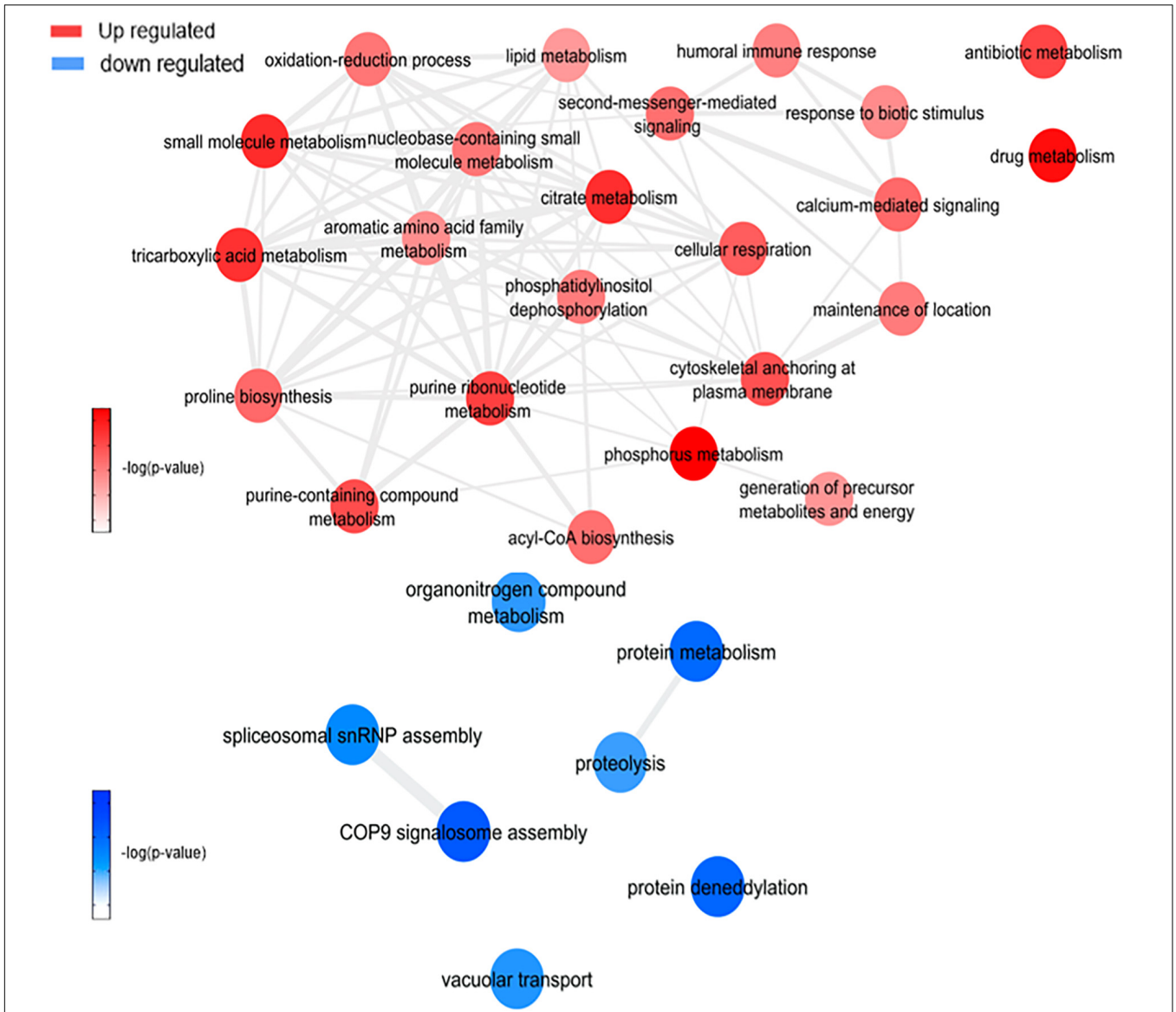

FIGURE 7 | Overview of significantly enriched GO [–log10 (*P*-value)] terms of ontological interaction network in biological processes of up-regulated (red) and down-regulated (blue) genes in coinfected mosquitoes versus ZIKV infected mosquitoes.

to ZIKV infection. Koh et al. (2020) confirmed such behavior during co-infection-induced intracellular events with DENV and *Wolbachia*, suggesting that they do not compete by lipids in host cell and virus-driven modulation dominates over that of *Wolbachia* (Koh et al., 2020), which may have occurred as well as in our experiment. In contrast, there is a down-regulation in GDP-mannose proteins genes synthesis, which may suggest that host cells no longer produce glycoconjugates for bacteria use.

Within the up-regulated genes in WZ compared to Z, ATP synthesis (ATPase subunit O; AAEL010823-PA), and cytoskeleton dynamics like microtubule binding and associated-proteins (AAEL009375-PK, AAEL004176-PB, and AAEL009847-PB) suggest activation of the ubiquitin-proteasome system. Indeed, it was previously reported in *Drosophila* and mosquito cell lines transfected, that *Wolbachia* relies on host proteolysis through ubiquitination to acquire essential amino acid for the infection (Fallon and Witthuhn, 2009; White et al., 2017). Flavivirus also need a functioning ubiquitin-proteasome system to complete their life cycle (Choy et al., 2015a,b), however, Ub3881 (AAEL003881), a ubiquitin-protein, is highly down-regulated in mosquitoes infected with DENV and its overexpression was able to control the virus infection (Troupin et al., 2016). In our analysis, we identified a paralog of the Ub3881 ubiquitin protein (AAEL003888), which was up-regulated in WZ versus Z and down-regulated in Z, suggesting that *Wolbachia* have a role in AAEL003888 expression enhancement which might target the

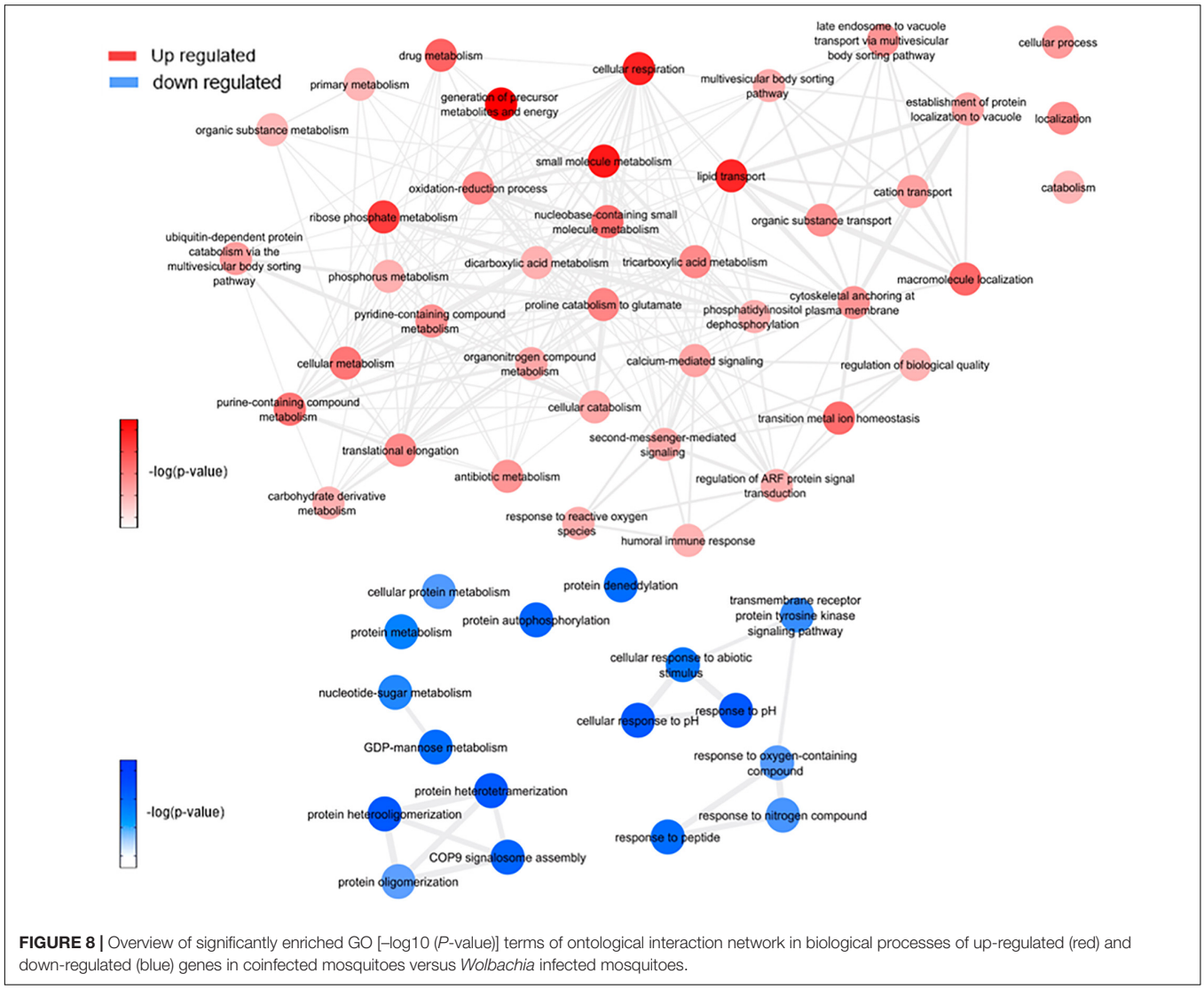

FIGURE 8 | Overview of significantly enriched GO [–log10 (*P*-value)] terms of ontological interaction network in biological processes of up-regulated (red) and down-regulated (blue) genes in coinfected mosquitoes versus *Wolbachia* infected mosquitoes.

envelope proteins of ZIKV for degradation, therefore hindering the virus assembly.

Exploring neuropeptides and hormones, neuropeptide sulfakinin (SK) (AAEL006451-PB) and insulin-like peptide (ILP) 1 (AAEL000937-PA) were down-regulated comparing WZ with Z. SK are a family of neuropeptides, homologous to mammalian gastrin/cholecystokinin (CCK), responsible for food uptake control in insects (Zels et al., 2015) while ILPs are known for signaling carbohydrates intake in cells (Nässel and Broeck, 2016). A recent study correlated SK influence in ILPs concentration, where a rise in SK concentration promotes ILPs production (Słocińska et al., 2020). SK down-regulation, observed in our data, may decrease in mosquito feeding satisfaction. This fact allied to ILP down-regulation, leading to a decrease in glycolysis cell assimilation, can be understood as a virus-infection influence to increase mosquito blood uptake, elevating ZIKV transmission success.

There are several processes up-regulated after enrichment comparison between WZ and Z. Cellular respiration, aerobic respiration, small molecule metabolic process, tricarboxylic acid cycle, oxidative phosphorylation, ATP synthesis coupled electron transport, respiratory electron transport chain, generation of precursor metabolites and energy, tricarboxylic acid metabolic process, nicotinamide nucleotide metabolic process, and cellular process were enriched up-regulated biological process by proteins genes ATP-citrate synthase (AAEL004297), glutamate semialdehyde dehydrogenase (AAEL006834), ATP synthase delta chain (AAEL010823), phosphatidylinositol-4,5-bisphosphate 4-phosphatase (AAEL011216), NADH-ubiquinone oxidoreductase (AAEL012552), mitochondrial aconitase (AAEL012897), 4-hydroxyphenylpyruvate dioxygenase (AAEL014600), titin (AAEL002565), and myosin (AAEL000596) up-regulation. The increase in aerobic respiration metabolism in *Wolbachia* infection proved to stimulate ROS production in insect cells as part of the host immune response, but it counterbalances with antioxidant pathways activation (Zug and Hammerstein, 2015). However, it was observed in WZ that the aerobic metabolism increases together with transition metal ions biological process

and pathways, mediated by putative secreted ferritin G subunit precursor (AAEL007383) and transferrin (AAEL015458), which can also generate ROS (Liu et al., 2016). ROS likely activates the Toll-immune pathway to confront ZIKV, similar to DENV infection (Selivanov et al., 2008). Also, two eukaryotic elongation factor 1-alpha (eEF1A) proteins (AAEL017096; AAEL017301) were up-regulated comparing WZ and Z. eEF1A increase was described as a response to endoplasmic reticulum stress caused by ROS in Chinese hamster ovary (Borradaile et al., 2005), which may have occurred in the mosquito. Another observed data was SRPN25 down-regulated in WZ, which was up-regulated in W. SRPN25 down-regulation in WZ highlights its function related to the insect immune system. Serpins can block the Toll signaling cascade and β-1,3-glucan-mediated melanin biosynthesis (Jiang et al., 2009), so its downregulation can infer that the insect immune system is activated.

This led us to understand insects defense mechanisms, induced by the presence of endosymbiotic bacteria, that may have been acting against virus infection: melanization activation mediated by SRPN25 down-regulation and Toll-pathway with the influence of SPRN25 down-regulation and the exacerbated production of ROS by aerobic metabolism increase. ROS occurs inside the mitochondria, after the oxidative phosphorylation stage, which has oxygen as the final electron acceptor, forming metabolic water. When oxygen is prematurely and incompletely reduced, it gives rise to superoxide anion, classified as ROS, together with hydrogen peroxide, hypochlorous acid, hydroxyl radical, singlet oxygen, and ozone (Lambert and Brand, 2009). Pan et al. described the relation between *Wolbachia* presence in *A. aegypti* and Toll-pathway activation by ROS to control DENV (Pan et al., 2012). This study not only confirms oxidative stress caused by Wolbachia, but also antioxidant genes expression as described earlier in this article. The role of symbiotic microorganisms in arbovirus infection of arthropods vectors is widely discussed, highlighting the importance of a ROS-mediated stimulation of the Toll-pathway and AMPs expression (Yin et al., 2020). As SPRN25 is down-regulated, serpins activity is up-regulated, which lead to serpins key response in the defense mechanism of insects, activating especially the Toll pathway, as well as ROS, and prophenoloxidase (PPO) cascade (Meekins et al., 2017). As for PPO cascade, it mediates melanization immune response in insects, including mosquito vectors (Christensen et al., 2005), It was already investigated that melanization suppression by SRPN activation can lead to a increase in viral infection (Toufeeq et al., 2019), calling attention to SRPN importance in mosquito immune response.

CONCLUSION

Proteomics analysis of female's head of *A. aegypti* during mono-infection with ZIKV or *Wolbachia* highlighted how those microorganisms use cell host for their benefits. Our data support that ZIKV may induces lipid synthesis and transport allied with glycolysis pathways while *Wolbachia* increases glycoconjugates production. During co-infection, *Wolbachia* probably helps *A. aegypti* to prevent virus infection by stimulating ROS production leading to Toll-pathway humoral immune response, together with antioxidant production to control cell homeostasis. This mechanism seems to be efficient since we have shown that peptides coming from the ZIKV polyprotein are reduced in female's heads of *A. aegypti* in the presence of *Wolbachia*. Our study has provided important insights into the differential manner in which *A. aegypti* proteome is systemically regulated during mono- and co-infections of ZIKV and *Wolbachia*. Ultimately, this work represents a rich resource for the insect research community to help elucidate the mechanisms by which *Wolbachia* orchestrate resistance to ZIKV infection in *A. aegypti* and it allows the generation of specific hypothesis-driven experiments in future studies.

DATA AVAILABILITY STATEMENT

The data presented in the study are deposited in the Proteome X Change repository, accession number PXD022665.

AUTHOR CONTRIBUTIONS

MM, LR, JM, AT, and SC performed the experiments and data analysis. MM and SC produced manuscript figures. MM, LR, JM, AT, SC, GD, DO, RM, FN, RM-D-F, and MJ wrote the manuscript. RM-D-F and MJ idealized and coordinated the study. All authors approved the manuscript.

FUNDING

The present work was supported by the Fundação Carlos Chagas Filho de Amparo à Pesquisa do Estado do Rio de Janeiro (FAPERJ) and Conselho Nacional de Desenvolvimento Científico e Tecnológico (CNPq).

ACKNOWLEDGMENTS

The authors thank Fabio Mendonça Gomes from Instituto de Biofísica Carlos Chagas Filho – UFRJ and Livia Goto-Silva from D'Or Institute for Research and Education (IDOR) for their critical reading of the manuscript.

SUPPLEMENTARY MATERIAL

The Supplementary Material for this article can be found online at: https://www.frontiersin.org/articles/10.3389/fphys.2021.642237/full#supplementary-material

REFERENCES

Aebersold, R., and Mann, M. (2016). Mass-spectrometric exploration of proteome structure and function. *Nature* 537, 347–355. doi: 10.1038/nature19949

Aliota, M. T., Walker, E. C., Yepes, A. U., Velez, I. D., Christensen, B. M., and Osorio, J. E. (2016). The wMel strain of Wolbachia reduces transmission of Chikungunya virus in *Aedes aegypti*. *PLoS Negl. Trop. Dis.* 10:e0004677. doi: 10.1371/journal.pntd.0004677

Ashburner, M., Ball, C. A., Blake, J. A., Botstein, D., Butler, H., Cherry, J. M., et al. (2000). Gene ontology: tool for the unification of biology. *Nat. Genet.* 25, 25–29. doi: 10.1038/75556

Barreto, M. L., Barral-Netto, M., Stabeli, R., Almeida-Filho, N., Vasconcelos, P. F. C., Teixeira, M., et al. (2016). Zika virus and microcephaly in Brazil: a scientific agenda. *Lancet* 387, 919–921. doi: 10.1016/S0140-6736(16)00545-6

Baud, D., Gubler, D. J., Schaub, B., Lanteri, M. C., and Musso, D. (2017). An update on Zika virus infection. *Lancet* 390, 2099–2109. doi: 10.1016/S0140-6736(17)31450-2

Borradaile, N. M., Buhman, K. K., Listenberger, L. L., Magee, C. J., Morimoto, E. T. A., Ory, D. S., et al. (2005). A critical role for eukaryotic elongation factor 1A-1 in lipotoxic cell death. *MBoC* 17, 770–778. doi: 10.1091/mbc.e05-08-0742

Brennan, L. J., Keddie, B. A., Braig, H. R., and Harris, H. L. (2008). The endosymbiont *Wolbachia pipientis* induces the expression of host antioxidant proteins in an *Aedes albopictus* cell line. *PLoS One* 3:e2083. doi: 10.1371/journal.pone.0002083

Calvo, E., Mizurini, D. M., Sá-Nunes, A., Ribeiro, J. M. C., Andersen, J. F., Mans, B. J., et al. (2011). Alboserpin, a factor Xa inhibitor from the mosquito vector of yellow fever, binds heparin and membrane phospholipids and exhibits antithrombotic activity. *J. Biol. Chem.* 286, 27998–28010. doi: 10.1074/jbc.M111.247924

Caminati, G., and Procacci, P. (2020). Mounting evidence of FKBP12 implication in neurodegeneration. *Neural Regen. Res.* 15, 2195–2202. doi: 10.4103/1673-5374.284980

Campos, G., Bandeira, A., and Sardi, S. (2015). Zika virus outbreak, Bahia, Brazil. *Emerg. Infect. Dis. J.* 21:1885. doi: 10.3201/eid2110.150847

Cheon, H.-M., Shin, S. W., Bian, G., Park, J.-H., and Raikhel, A. S. (2006). Regulation of lipid metabolism genes, lipid carrier protein lipophorin, and its receptor during immune challenge in the mosquito *Aedes aegypti*. *J. Biol. Chem.* 281, 8426–8435. doi: 10.1074/jbc.M510957200

Chisenhall, D. M., Londono, B. L., Christofferson, R. C., McCracken, M. K., and Mores, C. N. (2014). Effect of dengue-2 virus infection on protein expression in the salivary glands of *Aedes aegypti* mosquitoes. *Am. J. Trop. Med. Hyg.* 90, 431–437. doi: 10.4269/ajtmh.13-0412

Choudhary, C., and Mann, M. (2010). Decoding signalling networks by mass spectrometry-based proteomics. *Nat. Rev. Mol. Cell Biol.* 11, 427–439. doi: 10.1038/nrm2900

Chouin-Carneiro, T., Vega-Rua, A., Vazeille, M., Yebakima, A., Girod, R., Goindin, D., et al. (2016). Differential susceptibilities of *Aedes aegypti* and *Aedes albopictus* from the Americas to Zika Virus. *PLoS Negl. Trop. Dis.* 10:e0004543. doi: 10.1371/journal.pntd.0004543

Choy, M. M., Sessions, O. M., Gubler, D. J., and Ooi, E. E. (2015a). Production of infectious dengue virus in *Aedes aegypti* is dependent on the ubiquitin proteasome pathway. *PLoS Negl. Trop. Dis.* 9:e0004227. doi: 10.1371/journal.pntd.0004227

Choy, M. M., Zhang, S. L., Costa, V. V., Tan, H. C., Horrevorts, S., and Ooi, E. E. (2015b). Proteasome inhibition suppresses dengue virus egress in antibody dependent infection. *PLoS Negl. Trop. Dis.* 9:e0004058. doi: 10.1371/journal.pntd.0004058

Christensen, B. M., Li, J., Chen, C.-C., and Nappi, A. J. (2005). Melanization immune responses in mosquito vectors. *Trends Parasitol.* 21, 192–199. doi: 10.1016/j.pt.2005.02.007

Codeço, C. T., Lima, A. W. S., Araújo, S. C., Lima, J. B. P., Maciel-de-Freitas, R., Honório, N. A., et al. (2015). Surveillance of *Aedes aegypti*: comparison of house index with four alternative traps. *PLoS Negl. Trop. Dis.* 9:e0003475. doi: 10.1371/journal.pntd.0003475

Cui, Y., Liu, P., Mooney, B. P., and Franz, A. W. E. (2020). Quantitative proteomic analysis of Chikungunya virus-infected *Aedes aegypti* reveals proteome modulations indicative of persistent infection. *J. Proteome Res.* 19, 2443–2456. doi: 10.1021/acs.jproteome.0c00173

da Rocha Fernandes, M., Martins, R., Pessoa Costa, E., Pacidônio, E. C., Araujo, et al. (2014). The modulation of the symbiont/host interaction between *Wolbachia pipientis* and *Aedes fluviatilis* embryos by glycogen metabolism. *PLoS One* 9:e98966. doi: 10.1371/journal.pone.0098966

da Silveira, I. D., Petersen, M. T., Sylvestre, G., Garcia, G. A., David, M. R., Pavan, M. G., et al. (2018). Zika virus infection produces a reduction on *Aedes aegypti* lifespan but no effects on mosquito fecundity and oviposition success. *Front. Microbiol.* 9:3011. doi: 10.3389/fmicb.2018.03011

De Mandal, S., Lin, B., Shi, M., Li, Y., Xu, X., and Jin, F. (2020). iTRAQ-based comparative proteomic analysis of larval midgut from the beet armyworm, *Spodoptera exigua* (Hübner) (Lepidoptera: Noctuidae) challenged with the entomopathogenic bacteria *Serratia marcescens*. *Front. Physiol.* 11:442. doi: 10.3389/fphys.2020.00442

Dhawan, R., Mohanty, A. K., Kumar, M., Dey, G., Advani, J., Prasad, T. S. K., et al. (2017). Data from salivary gland proteome analysis of female *Aedes aegypti* Linn. *Data Brief.* 13, 274–277. doi: 10.1016/j.dib.2017.05.034

Dick, G. W. A., Kitchen, S. F., and Haddow, A. J. (1952). Zika Virus (I). Isolations and serological specificity. *Trans. R. Soc. Trop. Med. Hyg.* 46, 509–520. doi: 10.1016/0035-9203(52)90042-4

Duncan, A. B., Agnew, P., Noel, V., Demettre, E., Seveno, M., Brizard, J.-P., et al. (2012). Proteome of *Aedes aegypti* in response to infection and coinfection with microsporidian parasites. *Ecol. Evol.* 2, 681–694. doi: 10.1002/ece3.199

Dutra, H. L. C., Rocha, M. N., Dias, F. B. S., Mansur, S. B., Caragata, E. P., and Moreira, L. A. (2016). Wolbachia blocks currently circulating Zika virus isolates in Brazilian *Aedes aegypti* mosquitoes. *Cell Host Microbe* 19, 771–774. doi: 10.1016/j.chom.2016.04.021

El-Bacha, T., and Da Poian, A. T. (2013). Virus-induced changes in mitochondrial bioenergetics as potential targets for therapy. *Int. J. Biochem. Cell Biol.* 45, 41–46. doi: 10.1016/j.biocel.2012.09.021

El-Gebali, S., Mistry, J., Bateman, A., Eddy, S. R., Luciani, A., Potter, S. C., et al. (2018). The Pfam protein families database in 2019. *Nucleic Acids Res.* 47, 427–432. doi: 10.1093/nar/gky995

Fallon, A. M., and Witthuhn, B. A. (2009). Proteasome activity in a naïve mosquito cell line infected with *Wolbachia pipientis* wAlbB. *Vitro Cell. Dev. Biol. Anim.* 45, 460–466. doi: 10.1007/s11626-009-9193-6

Fernandes, R. S., Campos, S. S., Ferreira-de-Brito, A., Miranda, R. M., Barbosa, da Silva, K. A., et al. (2016). *Culex quinquefasciatus* from Rio de janeiro is not competent to transmit the local Zika Virus. *PLoS Negl. Trop. Dis.* 10:e0004993. doi: 10.1371/journal.pntd.0004993

Ferreira-de-Brito, A., Ribeiro, I. P., Miranda, R. M., Fernandes, R. S., Campos, S. S., Silva, K. A., et al. (2016). First detection of natural infection of *Aedes aegypti* with Zika virus in Brazil and throughout South America. *Memórias Instit. Oswaldo Cruz* 111, 655–658. doi: 10.1590/0074-02760160332

Fitzgerald, K. A., and Kagan, J. C. (2020). Toll-like receptors and the control of immunity. *Cell* 180, 1044–1066. doi: 10.1016/j.cell.2020.02.041

Ford, S. A., Albert, I., Allen, S. L., Chenoweth, S. F., Jones, M., Koh, C., et al. (2020). Artificial selection finds new hypotheses for the mechanism of Wolbachia-Mediated dengue blocking in mosquitoes. *Front. Microbiol.* 11:1456. doi: 10.3389/fmicb.2020.01456

Garcia, G. A., Sylvestre, G., Aguiar, R., da Costa, G. B., Martins, A. J., Lima, J. B. P., et al. (2019). Matching the genetics of released and local *Aedes aegypti* populations is critical to assure Wolbachia invasion. *PLoS Negl. Trop. Dis.* 13:e0007023. doi: 10.1371/journal.pntd.0007023

García-Robles, I., De Loma, J., Capilla, M., Roger, I., Boix-Montesinos, P., Carrión, P., et al. (2020). Proteomic insights into the immune response of the Colorado potato beetle larvae challenged with *Bacillus thuringiensis*. *Dev. Comp. Immunol.* 104:103525. doi: 10.1016/j.dci.2019.103525

García-del Portillo, F. (2020). Building peptidoglycan inside eukaryotic cells: a view from symbiotic and pathogenic bacteria. *Mol. Microbiol.* 113, 613–626. doi: 10.1111/mmi.14452

Geoghegan, V., Stainton, K., Rainey, S. M., Ant, T. H., Dowle, A. A., Larson, T., et al. (2017). Perturbed cholesterol and vesicular trafficking associated with dengue blocking in Wolbachia -infected *Aedes aegypti* cells. *Nat. Commun.* 8:526. doi: 10.1038/s41467-017-00610-8

Giraldo-Calderón, G. I., Emrich, S. J., MacCallum, R. M., Maslen, G., Dialynas, E., Topalis, P., et al. (2015). VectorBase: an updated bioinformatics resource for invertebrate vectors and other organisms related with human diseases. *Nucleic Acids Res.* 43, 707–713. doi: 10.1093/nar/gku1117

Guo, J., Jia, X., Liu, Y., Wang, S., Cao, J., Zhang, B., et al. (2020). Inhibition of Na + /K + ATPase blocks Zika virus infection in mice. *Commun. Biol.* 3, 380. doi: 10.1038/s42003-020-1109-8

Guo, X., Wu, S., Li, N., Lin, Q., Liu, L., Liang, H., et al. (2019). Accelerated metabolite levels of aerobic glycolysis and the pentose phosphate pathway are required for efficient replication of infectious spleen and kidney necrosis virus in chinese perch brain cells. *Biomolecules* 9:440. doi: 10.3390/biom9090440

Haqshenas, G., Terradas, G., Paradkar, P. N., Duchemin, J.-B., McGraw, E. A., and Doerig, C. (2019). A role for the insulin receptor in the suppression of dengue virus and Zika virus in wolbachia-infected mosquito cells. *Cell Rep.* 26, 529.e3–535.e3. doi: 10.1016/j.celrep.2018.12.068

Hoffmann, A. A., Montgomery, B. L., Popovici, J., Iturbe-Ormaetxe, I., Johnson, P. H., Muzzi, F., et al. (2011). Successful establishment of Wolbachia in Aedes populations to suppress dengue transmission. *Nature* 476, 454–457. doi: 10.1038/nature10356

Holt, R. A., Subramanian, G. M., Halpern, A., Sutton, G. G., Charlab, R., Nusskern, D. R., et al. (2002). The genome sequence of the malaria mosquito *Anopheles gambiae*. *Science* 298, 129–149. doi: 10.1126/science.1076181

Hong, W., Mo, F., Zhang, Z., Huang, M., and Wei, X. (2020). Nicotinamide mononucleotide: a promising molecule for therapy of diverse diseases by targeting NAD+ metabolism. *Front. Cell Dev. Biol.* 8:246. doi: 10.3389/fcell.2020.00246

Indriani, C., Tantowijoyo, W., Rancès, E., Andari, B., Prabowo, E., Yusdi, D., et al. (2020). Reduced dengue incidence following deployments of Wolbachia-infected *Aedes aegypti* in Yogyakarta, Indonesia: a quasi-experimental trial using controlled interrupted time series analysis. *Gates Open Res.* 4:50. doi: 10.12688/gatesopenres.13122.1

Jiang, R., Kim, E.-H., Gong, J.-H., Kwon, H.-M., Kim, C.-H., Ryu, K.-H., et al. (2009). Three pairs of protease-serpin complexes cooperatively regulate the insect innate immune responses. *J. Biol. Chem.* 284, 35652–35658. doi: 10.1074/jbc.M109.071001

Kingsolver, M. B., Huang, Z., and Hardy, R. W. (2013). Insect antiviral innate immunity: pathways, effectors, and connections. *J. Mol. Biol.* 425, 4921–4936. doi: 10.1016/j.jmb.2013.10.006

Koh, C., Islam, M. N., Ye, Y. H., Chotiwan, N., Graham, B., Belisle, J. T., et al. (2020). Dengue virus dominates lipid metabolism modulations in Wolbachia - coinfected *Aedes aegypti*. *Commun. Biol.* 3:e0007443. doi: 10.1038/s42003-020-01254-z

Kumar, A., Prasad, A., Sedlářová, M., Ksas, B., Havaux, M., and Pospíšil, P. (2020). Interplay between antioxidants in response to photooxidative stress in *Arabidopsis*. *Free Radic. Biol. Med.* 160, 894–907. doi: 10.1016/j.freeradbiomed.2020.08.027

Kuzmina, N. V., Loshkareva, A. S., Shilova, L. A., Shtykova, E. V., Knyazev, D. G., Zimmerberg, J., et al. (2020). Protein-lipid interactions in formation of viral envelopes. *Biophys. J.* 118:523a. doi: 10.1016/j.bpj.2019.11.2874

Lambert, A. J., and Brand, M. D. (2009). "Reactive oxygen species production by mitochondria," in *Mitochondrial DNA: Methods and Protocols Methods in Molecular Biology*^{TM}, ed. J. A. Stuart (Totowa, NJ: Humana Press), 165–181. doi: 10.1007/978-1-59745-521-3_11

Li, F., Zhao, X., Zhu, S., Wang, T., Li, T., Woolfley, T., et al. (2020). Identification and expression profiling of neuropeptides and neuropeptide receptor genes in *Atrijuglans hetaohei*. *Gene* 743:144605. doi: 10.1016/j.gene.2020.144605

Linthicum, K. J., Platt, K., Myint, K. S., Lerdthusnee, K., Inni, B. L., and Ghn, D. W. V. (1996). Dengue 3 virus distribution in the mosquito *Aedes aegypti*: an immunocytochemical study. *Medic. Vet. Entomol.* 10, 87–92. doi: 10.1111/j.1365-2915.1996.tb00086.x

Liu, K., Gao, Y., Liu, J., Wen, Y., Zhao, Y., Zhang, K., et al. (2016). Photoreactivity of metal–organic frameworks in aqueous solutions: metal dependence of reactive oxygen species production. *Environ. Sci. Technol.* 50, 3634–3640. doi: 10.1021/acs.est.5b06019

MaitiDutta, S., Chen, G., and Maiti, S. (2020). Tocopherol moderately induces the expressions of some human sulfotransferases, which are activated by oxidative stress. *Cell Biochem. Biophys.* 78, 439–446. doi: 10.1007/s12013-020-00938-x

Manokaran, G., Flores, H. A., Dickson, C. T., Narayana, V. K., Kanojia, K., Dayalan, S., et al. (2020). Modulation of acyl-carnitines, the broad mechanism behind Wolbachia-mediated inhibition of medically important flaviviruses in *Aedes aegypti*. *PNAS* 117, 24475–24483. doi: 10.1073/pnas.1914814117

Martín-Acebes, M. A., Vázquez-Calvo, Á, and Saiz, J.-C. (2016). Lipids and flaviviruses, present and future perspectives for the control of dengue, Zika, and West Nile viruses. *Prog. Lipid Res.* 64, 123–137. doi: 10.1016/j.plipres.2016.09.005

Meekins, D. A., Kanost, M. R., and Michel, K. (2017). Serpins in arthropod biology. *Semin. Cell Dev. Biol.* 62, 105–119. doi: 10.1016/j.semcdb.2016.09.001

Minter, B. E., Lowes, D. A., Webster, N. R., and Galley, H. F. (2020). Differential effects of MitoVitE, α-Tocopherol and Trolox on oxidative stress, mitochondrial function and inflammatory signalling pathways in endothelial cells cultured under conditions mimicking sepsis. *Antioxidants* 9:195. doi: 10.3390/antiox9030195

Moreira, L. A., Iturbe-Ormaetxe, I., Jeffery, J. A., Lu, G., Pyke, A. T., Hedges, L. M., et al. (2009). A Wolbachia symbiont in *Aedes aegypti* limits infection with dengue, chikungunya, and plasmodium. *Cell* 139, 1268–1278. doi: 10.1016/j.cell.2009.11.042

Murillo, J. R., Goto-Silva, L., Sánchez, A., Nogueira, F. C. S., Domont, G. B., and Junqueira, M. (2017). Quantitative proteomic analysis identifies proteins and pathways related to neuronal development in differentiated SH-SY5Y neuroblastoma cells. *EuPA Open Proteom.* 16, 1–11. doi: 10.1016/j.euprot.2017.06.001

Nässel, D. R., and Broeck, J. V. (2016). Insulin/IGF signaling in *Drosophila* and other insects: factors that regulate production, release and post-release action of the insulin-like peptides. *Cell. Mol. Life Sci.* 73, 271–290. doi: 10.1007/s00018-015-2063-3

Nazni, W. A., Hoffmann, A. A., NoorAfizah, A., Cheong, Y. L., Mancini, M. V., Golding, N., et al. (2019). Establishment of Wolbachia strain wAlbB in Malaysian populations of *Aedes aegypti* for dengue control. *Curr. Biol.* 29, 4241.e5–4248.e5. doi: 10.1016/j.cub.2019.11.007

Nowicka, B., Fesenko, T., Walczak, J., and Kruk, J. (2020). The inhibitor-evoked shortage of tocopherol and plastoquinol is compensated by other antioxidant mechanisms in *Chlamydomonas reinhardtii* exposed to toxic concentrations of cadmium and chromium ions. *Ecotoxicol. Environ. Saf.* 191:110241. doi: 10.1016/j.ecoenv.2020.110241

Nunes, A. T., Brito, N. F., Oliveira, D. S., Araujo, G. D. T., Nogueira, F. C. S., Domont, G. B., et al. (2016). Comparative proteome analysis reveals that blood and sugar meals induce differential protein expression in *Aedes aegypti* female heads. *Proteomics* 16, 2582–2586. doi: 10.1002/pmic.201600126

Paingankar, M. S., Gokhale, M. D., Deobagkar, D. D., and Deobagkar, D. N. (2020). *Drosophila melanogaster* as a model host to study arbovirus–vector interaction. *bioRxiv* doi: 10.1101/2020.09.03.282350

Pan, X., Zhou, G., Wu, J., Bian, G., Lu, P., Raikhel, A. S., et al. (2012). Wolbachia induces reactive oxygen species (ROS)-dependent activation of the Toll pathway to control dengue virus in the mosquito *Aedes aegypti*. *PNAS* 109, E23–E31. doi: 10.1073/pnas.1116932108

Pappireddi, N., Martin, L., and Wühr, M. (2019). A review on quantitative multiplexed proteomics. *ChemBioChem* 20, 1210–1224. doi: 10.1002/cbic.201800650

Perera, R., Riley, C., Isaac, G., Hopf-Jannasch, A. S., Moore, R. J., Weitz, K. W., et al. (2012). Dengue virus infection perturbs lipid homeostasis in infected mosquito cells. *PLoS Pathog.* 8:e1002584. doi: 10.1371/journal.ppat.1002584

Petersen, M. T., da Silveira, I. D., Tátila-Ferreira, A., David, M. R., Chouin-Carneiro, T., Van den Wouwer, L., et al. (2018). The impact of the age of first blood meal and Zika virus infection on *Aedes aegypti* egg production and longevity. *PLoS One* 13:e0200766. doi: 10.1371/journal.pone.0200766

Phillips, D. R., and Clark, K. D. (2017). *Bombyx mori* and *Aedes aegypti* form multi-functional immune complexes that integrate pattern recognition, melanization, coagulants, and hemocyte recruitment. *PLoS One* 12:e0171447. doi: 10.1371/journal.pone.0171447

Pickett, B. E., Sadat, E. L., Zhang, Y., Noronha, J. M., Squires, R. B., Hunt, V., et al. (2012). ViPR: an open bioinformatics database and analysis resource for virology research. *Nucleic Acids Res.* 40, D593–D598. doi: 10.1093/nar/gkr859

Poddar, S. K., Sifat, A. E., Haque, S., Nahid, N. A., Chowdhury, S., and Mehedi, I. (2019). Nicotinamide mononucleotide: exploration of diverse therapeutic applications of a potential molecule. *Biomolecules* 9:34. doi: 10.3390/biom9010034

Predel, R., Neupert, S., Garczynski, S. F., Crim, J. W., Brown, M. R., Russell, W. K., et al. (2010). Neuropeptidomics of the mosquito *Aedes aegypti*. *J. Proteome Res.* 9, 2006–2015. doi: 10.1021/pr901187p

Rauniyar, N., and Yates, J. R. (2014). Isobaric labeling-based relative quantification in shotgun proteomics. *Proteome Res.* 13, 5293–5309. doi: 10.1021/pr500880b

Rexer, T., Laaf, D., Gottschalk, J., Frohnmeyer, H., Rapp, E., and Elling, L. (2020). "Enzymatic synthesis of glycans and glycoconjugates," in *Advances in Biochemical Engineering/Biotechnology*, (Berlin: Springer), 1–50. doi: 10.1007/10_2020_148

Ribeiro, J. M. C., Martin-Martin, I., Arcà, B., and Calvo, E. (2016). A deep insight into the sialome of male and female *Aedes aegypti* mosquitoes. *PLoS One* 11:e0151400. doi: 10.1371/journal.pone.0151400

Ryan, P. A., Turley, A. P., Wilson, G., Hurst, T. P., Retzki, K., Brown-Kenyon, J., et al. (2020). Establishment of wMel Wolbachia in *Aedes aegypti* mosquitoes and reduction of local dengue transmission in cairns and surrounding locations in northern Queensland, Australia. *Gates Open Res.* 3:1547. doi: 10.12688/gatesopenres.13061.2

Schmid, M. A., Kauffman, E., Payne, A., Harris, E., and Kramer, L. D. (2017). Preparation of mosquito salivary gland extract and intradermal inoculation of mice. *Bio Protocol* 7:e2407.

Selivanov, V. A., Zeak, J. A., Roca, J., Cascante, M., Trucco, M., and Votyakova, T. V. (2008). The role of external and matrix pH in mitochondrial reactive oxygen species generation. *J. Biol. Chem.* 283, 29292–29300. doi: 10.1074/jbc.M801019200

Serteyn, L., Ponnet, L., Saive, M., Fauconnier, M.-L., and Francis, F. (2020). Changes of feeding behavior and salivary proteome of Brown Marmorated Stink Bug when exposed to insect-induced plant defenses. *Arthropod-Plant Interact.* 14, 101–112. doi: 10.1007/s11829-019-09718-8

Shrinet, J., Bhavesh, N. S., and Sunil, S. (2018). Understanding oxidative stress in aedes during chikungunya and dengue virus infections using integromics analysis. *Viruses* 10:314. doi: 10.3390/v10060314

Słocińska, M., Chowański, S., and Marciniak, P. (2020). Identification of sulfakinin receptors (SKR) in *Tenebrio molitor* beetle and the influence of sulfakinins on carbohydrates metabolism. *J. Comp. Physiol. B* 190, 669–679. doi: 10.1007/s00360-020-01300-6

Stark, K. R., and James, A. A. (1998). Isolation and characterization of the gene encoding a novel factor xa-directed anticoagulant from the yellow fever mosquito, *Aedes aegypti*. *J. Biol. Chem.* 273, 20802–20809. doi: 10.1074/jbc.273.33.20802

Sterkel, M., Perdomo, H. D., Guizzo, M. G., Barletta, A. B. F., Nunes, R. D., Dias, F. A., et al. (2016). Tyrosine detoxification is an essential trait in the life history of blood-feeding arthropods. *Curr. Biol.* 26, 2188–2193. doi: 10.1016/j.cub.2016.06.025

Stick, R. V., and Williams, S. J. (2009). "Chapter 11 - Glycoproteins and proteoglycans," in *Carbohydrates: The Essential Molecules of Life (Second Edition)*, eds R. V. Stick and S. J. Williams (Oxford: Elsevier), 369–412.

Supek, F., Bošnjak, M., Škunca, N., and Šmuc, T. (2011). REVIGO summarizes and visualizes long lists of gene ontology terms. *PLoS One* 6:e21800. doi: 10.1371/journal.pone.0021800

The Uniprot Consortium (2019). UniProt: a worldwide hub of protein knowledge. *Nucleic Acids Res.* 47, D506–D515. doi: 10.1093/nar/gky1049

Toufeeq, S., Wang, J., Zhang, S.-Z., Li, B., Hu, P., Zhu, L.-B., et al. (2019). Bmserpin2 is involved in BmNPV infection by suppressing melanization in *Bombyx mori*. *Insects* 10:399. doi: 10.3390/insects10110399

Troupin, A., Londono-Renteria, B., Conway, M. J., Cloherty, E., Jameson, S., Higgs, S., et al. (2016). A novel mosquito ubiquitin targets viral envelope protein for degradation and reduces virion production during dengue virus infection. *Biochim. Biophys. Acta Gen. Subj.* 1860, 1898–1909. doi: 10.1016/j.bbagen.2016.05.033

Turley, A. P., Moreira, L. A., O'Neill, S. L., and McGraw, E. A. (2009). Wolbachia infection reduces blood-feeding success in the dengue fever mosquito, *Aedes aegypti*. *PLoS Negl. Trop. Dis.* 3:e516. doi: 10.1371/journal.pntd.0000516

Tyanova, S., Temu, T., Sinitcyn, P., Carlson, A., Hein, M. Y., Geiger, T., et al. (2016). The Perseus computational platform for comprehensive analysis of (prote)omics data. *Nat. Methods* 13, 731–740. doi: 10.1038/nmeth.3901

Vasconcellos, A. F., Mandacaru, S. C., de Oliveira, A. S., Fontes, W., Melo, R. M., de Sousa, M. V., et al. (2020). Dynamic proteomic analysis of *Aedes aegypti* Aag-2 cells infected with Mayaro virus. *Parasit. Vect.* 13:297. doi: 10.1186/s13071-020-04167-2

Wang, X., Zhang, Y., Zhang, R., and Zhang, J. (2019). The diversity of pattern recognition receptors (PRRs) involved with insect defense against pathogens. *Curr. Opin. Insect Sci.* 33, 105–110. doi: 10.1016/j.cois.2019.05.004

Wasinpiyamongkol, L., Patramool, S., Luplertlop, N., Surasombatpattana, P., Doucoure, S., Mouchet, F., et al. (2010). Blood-feeding and immunogenic *Aedes aegypti* saliva proteins. *Proteomics* 10, 1906–1916. doi: 10.1002/pmic.200900626

White, P. M., Serbus, L. R., Debec, A., Codina, A., Bray, W., Guichet, A., et al. (2017). Reliance of Wolbachia on high rates of host proteolysis revealed by a genome-wide RNAi screen of Drosophila cells. *Genetics* 205, 1473–1488. doi: 10.1534/genetics.116.198903

Xi, Z., Ramirez, J. L., and Dimopoulos, G. (2008). The *Aedes aegypti* toll pathway controls dengue virus infection. *PLoS Pathog.* 4:e1000098. doi: 10.1371/journal.ppat.1000098

Yin, C., Sun, P., Yu, X., Wang, P., and Cheng, G. (2020). Roles of symbiotic microorganisms in arboviral infection of arthropod vectors. *Trends Parasitol.* 36, 607–615. doi: 10.1016/j.pt.2020.04.009

Zels, S., Dillen, S., Crabbé, K., Spit, J., Nachman, R. J., and Vanden Broeck, J. (2015). Sulfakinin is an important regulator of digestive processes in the migratory locust, *Locusta migratoria*. *Insect Biochem. Mol. Biol.* 61, 8–16. doi: 10.1016/j.ibmb.2015.03.008

Zug, R., and Hammerstein, P. (2015). Wolbachia and the insect immune system: what reactive oxygen species can tell us about the mechanisms of Wolbachia–host interactions. *Front. Microbiol.* 6:1201. doi: 10.3389/fmicb.2015.01201

Conflict of Interest: The authors declare that the research was conducted in the absence of any commercial or financial relationships that could be construed as a potential conflict of interest.